

This is the accepted manuscript made available via CHORUS. The article has been published as:

Transits of the QCD critical point

Yukinao Akamatsu, Derek Teaney, Fanglida Yan, and Yi Yin

Phys. Rev. C **100**, 044901 — Published 1 October 2019

DOI: [10.1103/PhysRevC.100.044901](https://doi.org/10.1103/PhysRevC.100.044901)

Transits of the QCD Critical Point

Yukinao Akamatsu,^{1,*} Derek Teaney,^{2,†} Fanglida Yan,^{2,‡} and Yi Yin^{3,§}

¹*Department of Physics, Osaka University, Toyonaka, Osaka 560-0043, Japan*

²*Department of Physics and Astronomy,*

Stony Brook University, Stony Brook, New York 11794, USA

³*Center for Theoretical Physics, Massachusetts Institute of Technology,
Cambridge, Massachusetts 02139, USA*

(Dated: September 9, 2019)

Abstract

We analyze the evolution of hydrodynamic fluctuations in a heavy ion collision as the system passes close to the QCD critical point. We introduce two small dimensionless parameters λ and Δ_s to characterize the evolution. λ compares the microscopic relaxation time (away from the critical point) to the expansion rate $\lambda \equiv \tau_0/\tau_Q$, and Δ_s compares the baryon to entropy ratio, n/s , to its critical value, $\Delta_s \equiv (n/s - n_c/s_c)/(n_c/s_c)$. We determine how the evolution of critical hydrodynamic fluctuations depends parametrically on λ and Δ_s . Finally, we use this parametric reasoning to estimate the critical fluctuations and correlation length for a heavy ion collision, and to give guidance to the experimental search for the QCD critical point.

* akamatsu@kern.phys.sci.osaka-u.ac.jp

† derek.teaney@stonybrook.edu

‡ yan.fanglida@stonybrook.edu

§ yyin3@mit.edu

I. INTRODUCTION

A. Overview and goals

The conjectured QCD critical point is a landmark point in the QCD phase diagram. This is the end point of a line of first-order phase transitions, which separates the Quark-Gluon Plasma (QGP) phase from hadronic matter. Due to the sign problem at finite baryon chemical potential, lattice QCD simulations have yet to confirm the existence of a critical point [1]. Nevertheless, the conjectured point in the phase diagram is theoretically well motivated, and has been found in various effective field theory models, see Refs. [2–4] for reviews. An intense experimental effort is underway to locate and to characterize the critical point through a beam energy scan (BES) of heavy ion collisions at the Relativistic Heavy Ion Collider (RHIC) [5, 6].

The experimental search for the QCD critical point will focus on fluctuations. The existence of a critical point in a heavy ion collision should lead to large correlations and enhanced fluctuations of conserved densities [7, 8]. These enhanced fluctuations should manifest themselves through the multiplicity fluctuations of the produced hadrons. However, the systems created in these nuclear collisions are rapidly expanding, and consequently thermodynamic fluctuations will not be fully equilibrated. In particular, it has been demonstrated previously that due to the expansion of the fireball and the physics of critical slowing down, the critical fluctuations can differ significantly from their equilibrium expectation [9, 10]. Further, in any real experiment the system will not pass directly through the critical point, and this again will limit the size of the critical fluctuations.

To quantify how the expansion of the system and missing the critical point will tame the critical fluctuations we will introduce two small parameters, λ and Δ_s , which characterize the evolution of the fireball:

$$\lambda \equiv \frac{\tau_0}{\tau_Q}, \quad (1)$$

$$\Delta_s \equiv \frac{n_c}{s_c} \left(\frac{s}{n} - \frac{s_c}{n_c} \right). \quad (2)$$

The first parameter λ is the product of the microscopic relaxation time away from the critical point τ_0 and the expansion rate $1/\tau_Q$ (more precise definitions of τ_0 and τ_Q are given below). The second parameter Δ_s quantifies the deviation of the baryon number to entropy ratio n/s from its critical value n_c/s_c during the adiabatic expansion of the system. A primary goal of the current study is to determine how the magnitude of the critical fluctuations depends parametrically on these two small parameters.

In perfect equilibrium, the hydrodynamic fluctuations in the energy density (for example) are given by the text book thermodynamic formula

$$\langle \delta e(t, \mathbf{x}) \delta e(t, \mathbf{y}) \rangle|_{\text{equilibrium}} = T^2 C_v \delta^{(3)}(\mathbf{x} - \mathbf{y}), \quad (3)$$

where C_v is the specific heat at constant volume. In Fourier space this says that all wavenumbers have equal amplitude

$$\langle \delta e(t, \mathbf{k}) \delta e(t, -\mathbf{k}') \rangle|_{\text{equilibrium}} = T^2 C_v (2\pi)^3 \delta^{(3)}(\mathbf{k} - \mathbf{k}'). \quad (4)$$

However, for an expanding system, even away from the critical point, the distribution of fluctuations will not follow this equilibrium form, since long wavelengths of conserved quantities take a long time to relax to equilibrium. The second goal of this paper is to determine

the wavelength which characterizes the enhanced specific heats near the critical point, and to specify how this wavelength depends on λ and Δ_s .

Away from the critical point, there is a length scale ℓ_{\max} where modes with wavelength longer than ℓ_{\max} fall out of equilibrium and reflect the expansion history rather than the equilibrium specific heat [11]. Indeed, the equilibration of hydrodynamic fluctuations is a diffusive process. The diffusion coefficient away from the critical point is of order $D_0 \sim \ell_0^2/\tau_0$ where τ_0 is the relaxation time introduced above, and ℓ_0 is a microscopic length. The maximum wavelength that can be equilibrated by diffusion over the total time τ_Q is¹

$$\ell_{\max}^2 \sim \ell_0^2 \left(\frac{\tau_Q}{\tau_0} \right), \quad (5)$$

or

$$\ell_{\max} \sim \frac{\ell_0}{\sqrt{\lambda}}. \quad (6)$$

There is insufficient time to equilibrate modes longer than ℓ_{\max} , and thus ℓ_{\max} provides a robust upper cutoff on the size of critically correlated domains in the expanding fireball.

Near a critical point the diffusion coefficient is not a constant value D_0 , but rapidly approaches zero. Thus the length scale characterizing critical domains is necessarily smaller than ℓ_{\max} . Modes with wavelength $\ell \ll \ell_{\max}$ (but still longer than ℓ_0) are equilibrated away from the critical point, but fall out of equilibrium as the system approaches the critical point. The emergent length scale, which arises from the competition between the expansion of the fireball and the diffusive equilibration of fluctuations, is known as the Kibble-Zurek length ℓ_{kz} . The Kibble-Zurek length is the correlation length at the time when the system falls out of equilibrium, and characterizes both the magnitude and distribution of fluctuations in an evolving critical system [12–15]. The importance of Kibble-Zurek length (and time) for the QCD critical point search has been identified in Ref. [16]. As we will see, the Kibble-Zurek length is of order

$$\ell_{\text{kz}} \sim \frac{\ell_0}{\lambda^{0.18}}, \quad (7)$$

leading to an interesting hierarchy of scales $\ell_0 \ll \ell_{\text{kz}} \ll \ell_{\max}$. Both ℓ_{\max} and ℓ_{kz} are estimated in the conclusions.

Beyond parametric estimates, we will determine the time evolution of hydrodynamic correlators (such as Eq. (3)) by evolving stochastic hydrodynamics for an expanding fluid in the vicinity of the QCD critical point. Specifically, following Ref. [11] (see also Ref. [17, 18]), we will write down and solve a set hydro-kinetic equations governing the evolution of hydrodynamic two point functions. The hydro-kinetic approach reformulates stochastic hydrodynamics as non-fluctuating hydrodynamics (describing a long wavelength background) coupled to a set of deterministic kinetic equations describing the phase space distribution of short wavelength thermodynamic fluctuations, see also Refs. [18, 19] for related developments. The hydro-kinetic formulation successfully describes non-trivial effects such as the hydrodynamic tails [11] and the renormalization of bulk viscosity [20], both of which are a consequence of the non-equilibrium evolution of thermodynamic fluctuations. We first extend this approach to a system with non-zero net baryon density, and then implement critical fluctuations as implied by the critical universality. We show how characteristic length scale ℓ_{kz} emerges from the hydro-kinetic equations for an expanding fireball. See also Refs. [21–24] for previous studies of critical fluctuations based on stochastic hydrodynamics.

¹ In Ref. [11] the length scale ℓ_{\max} is parametrized by the wavenumber $k_* \sim 1/\ell_{\max}$.

B. Setup and outline

1. Setup

Consider the hydrodynamic evolution of a single fluid cell of QCD matter passing close to the critical point. In the rest frame of the material, the entropy and baryon number densities follow the equations of ideal hydrodynamics

$$\partial_\tau s = -s \nabla \cdot u, \quad (8a)$$

$$\partial_\tau n = -n \nabla \cdot u, \quad (8b)$$

where τ is the proper time of the fluid cell and $\nabla \cdot u = \partial_\mu u^\mu$ is the expansion scalar. Since the system is close to the critical point only for a short period of time we may treat the expansion scalar as a constant, $\partial_\mu u^\mu \equiv 1/\tau_Q$. Indeed, τ_Q is of order the system's lifetime, while the time scales for the critical dynamics t_{kz} and t_{cr} will be parametrically smaller than τ_Q justifying this approximation a-posteriori.

We will also consider fluctuations of n and s around these time dependent background values. In order to reasonably separate the system into background and fluctuations near the critical point, the wavelength of background $\sim c_0 \tau_Q$ should be long compared to the correlation length of the fluctuations. (Here $c_0 = \ell_0/\tau_0$ is a typical velocity away from the critical point.) If this is the case, the background value can be accurately determined as an average of many uncorrelated domains. As we will see, in an expanding system the correlation length near the critical point grows to a size denoted ℓ_{kz} below, which is parametrically small compared to $c_0 \tau_Q$. This justifies the division into background and fluctuations a-posteriori.

The entropy per baryon s/n in Eq. (8) is constant in time. We will refer to relative deviation of s/n from s_c/n_c as the “detuning” parameter, Δ_s . Close to the critical point

$$\Delta_s \equiv \frac{n_c}{s_c} \left(\frac{s}{n} - \frac{s_c}{n_c} \right) \simeq \frac{\Delta s}{s_c} - \frac{\Delta n}{n_c}, \quad (9)$$

where Δn notates the deviation from the critical value

$$\Delta n \equiv n - n_c, \quad (10)$$

with an analogous notation for other quantities (e.g. $\Delta\mu \equiv \mu - \mu_c$). Δ_s is a dimensionless number and is small for a system passing close to the critical point.

There is a time τ_1 where the baryon number reaches its critical value, n_c . The entropy at this time differs from its critical value by $\Delta\bar{s}/s_c \simeq \Delta_s$. For times close to τ_1 , we can integrate the equations of motion Eq. (8) yielding

$$\frac{\Delta n(t)}{n_c} = -\frac{t}{\tau_Q}, \quad (11a)$$

$$\frac{\Delta s(t)}{s_c} = \Delta_s - \frac{t}{\tau_Q}, \quad (11b)$$

where we have defined $t \equiv \tau - \tau_1$. In writing Eq. (11) we have neglected terms of order $(t/\tau_Q)\Delta_s$ which contain two small parameters, t/τ_Q and Δ_s . Thermodynamics relates the deviation in the (average) energy density from its critical value to these two quantities

$$\Delta e = T_c \Delta s + \mu_c \Delta n. \quad (12)$$

In Fig. 1(a) we show a schematic picture of typical trajectory in the full QCD phase diagram, portrayed in the (n, s) -plane². In Fig. 1(b) we have rescaled the axes of (a) by n_c and s_c and expanded the region near the critical point. The detuning parameter Δ_s is the intercept of 45° lines which label the trajectories of the system. Finally, in Fig. 1(c) (which is discussed more completely in Sect. II C) we have rescaled the $\Delta n/n_c$ and $\Delta s/s_c$ axes of Fig. 1(b) by Δ_s and $\Delta_s^{(1-\alpha)/\beta}$ respectively. Only in (c) does the fact that the system misses the critical point by an amount Δ_s become important.

2. Computational outline

The goal of the current paper is to determine how the distribution of hydrodynamic fluctuations evolves in time as the mean entropy and baryon number densities evolve according to Eq. (11), and the system passes close to the critical point with parameter Δ_s . For several important (and related) reasons the primary object of study is the distribution of fluctuations in the entropy per baryon $\delta\hat{s} \equiv n\delta(s/n)$

$$N^{\hat{s}\hat{s}}(t, \mathbf{k}) \equiv \int d^3x e^{i\mathbf{k}\cdot(\mathbf{x}-\mathbf{y})} \langle \delta\hat{s}(t, \mathbf{x}) \delta\hat{s}(t, \mathbf{y}) \rangle. \quad (13)$$

First, this correlation function diverges near the critical point as the Ising magnetic susceptibility χ_{is} , which has the largest critical exponent $\gamma \simeq 1.23$ (see [26] and Sect. II B 3). Second, $N^{\hat{s}\hat{s}}$ determines the specific heat at constant pressure C_p in the limit $\mathbf{k} \rightarrow 0$ (see [27] and Sect. II B 2). Finally, the $\delta\hat{s}$ fluctuation is a diffusive eigen-mode of the linearized hydrodynamic equations, and therefore evolves independently of other hydrodynamic fluctuations. The associated heat diffusion coefficient $D_{\hat{s}}$, which controls the relaxation of $\delta\hat{s}$, is similar in magnitude to the baryon number diffusion coefficient D_B (see [28, 29] and Sect. III A 1). We will determine how the amplitude and the shape of the $N^{\hat{s}\hat{s}}$ distribution depend on the parameters λ and Δ_s .

We first need to describe how this correlation function would evolve in perfect equilibrium; this involves several ingredients as described in Sect. II. The time evolution of the overall amplitude of $N^{\hat{s}\hat{s}}$ in equilibrium is given by $C_p(t)$ which is related through universality to the Ising magnetic susceptibility χ_{is} . In Sect. II A we describe how to map the QCD quantities Δs and Δn onto the phase diagram of the Ising model. Since the time dependence of Δs and Δn has already been prescribed in Eq. (11), once the QCD-to-Ising map is given, the time evolution of $\chi(t) \propto C_p(t)$ is fixed. The shape of the $N^{\hat{s}\hat{s}}$ distribution is controlled by the correlation length $\xi(t)$ which is also specified through universality. In equilibrium, the relaxation time parameter λ plays no role, and the evolution of $N_0^{\hat{s}\hat{s}}$ is determined only by τ_Q and Δ_s . As we show in Sect. II C, the relevant timescale for the non-trivial evolution of $C_p(t)$ and $\xi(t)$ is set by a crossing timescale:

$$t_{\text{cr}} \sim \tau_Q \Delta_s^b, \quad b \equiv \frac{1-\alpha}{\beta} \simeq 2.7. \quad (14)$$

The equilibrium evolution of the $N^{\hat{s}\hat{s}}$ is summarized in Sect. II D, where the time dependence of the amplitude $C_p(t) \propto \chi_{\text{is}}(t)$ and correlation length $\xi(t)$ are shown in Fig. 2(a) and (b) respectively.

² In this figure the coexistence line is shown as a flat line, which is a commonly used idealization [25]. This idealization is not essential to the parametric reasoning discussed in the text and illustrated in Fig. 1

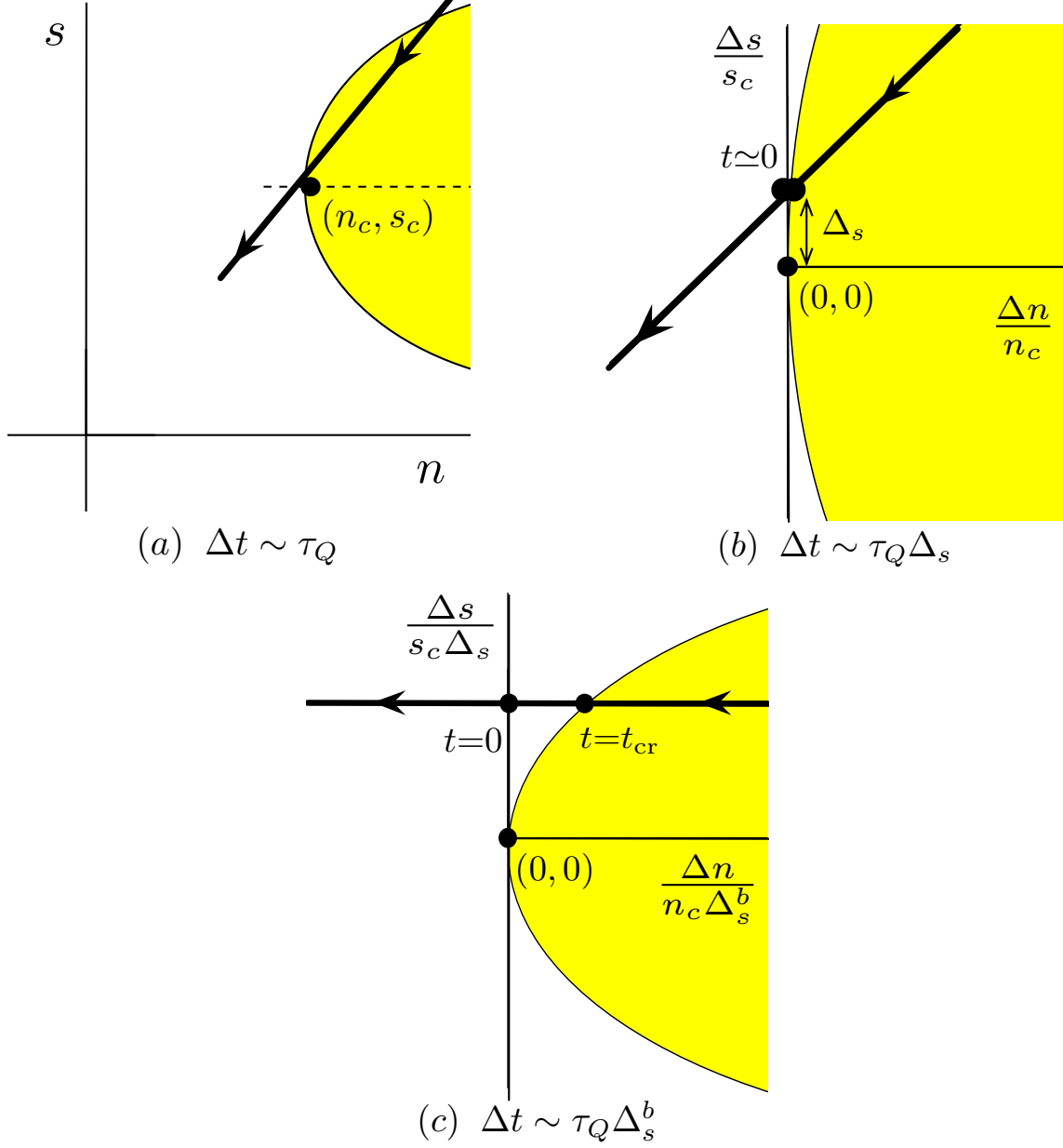


FIG. 1. (a) A schematic trajectory of a heavy ion collision passing close to the critical point. The duration of panel (a) is of order $\Delta t \sim \tau_Q$. (b) A magnification of the critical region in figure (a) by Δ_s . The duration of panel (b) is of order $\Delta t \sim \tau_Q \Delta_s$. In this regime the Ising magnetic field h is negligibly small, and the susceptibilities scale as a power $\Delta n/n_c$. (c) In this panel we have rescaled the $\Delta n/n_c$ and $\Delta s/s_c$ axes of (b) by Δ_s^b and Δ_s respectively, with $b \equiv (1 - \alpha)/\beta \simeq 2.7$. The duration of panel (c) is of order $\Delta t \sim t_{\text{cr}} \sim \tau_Q \Delta_s^b$. At the time t_{cr} the system leaves the coexistence region and the equilibrium correlation length reaches its maximal value (see Eq. (84)). Only in panel (c) is the equation of state is a nontrivial function (i.e. beyond simple powers) of the scaling variable $z \propto r/h^{1/\beta\delta}$.

After specifying how the equilibrium expectation evolves we will write down a dynamical evolution equation for $N^{\hat{s}\hat{s}}$ by analyzing stochastic hydrodynamics in the expanding critical background – see Sect. III. The diffusion coefficient entering in this evolution equation determines a relaxation rate $\Gamma_{\hat{s}}$ for the $\delta\hat{s}$ mode, which approaches zero near the critical point, $\Gamma_{\hat{s}} \propto \xi^{-z}$ with $z = 4 - \eta$. Comparing the relaxation rate to the rate of change of the equilibrium expectation yields an emergent Kibble-Zurek timescale

$$t_{\text{kz}} \sim \tau_Q \lambda^{-a\nu z/(1+a\nu z)}, \quad a \equiv \frac{1}{1-\alpha} \simeq a \simeq 1.12, \quad (15)$$

which sets the timescale for the non-equilibrium evolution of the fluctuations. The Kibble-Zurek time is described more completely in Sect. III C.

Our final numerical result for the time evolution of $N^{\hat{s}\hat{s}}$ when the system passes directly through the critical point ($t_{\text{cr}} = 0$) is shown in Fig. 3 of Sect. III D. When the system misses the critical $N^{\hat{s}\hat{s}}(t, \mathbf{k})$ generally depends on the ratio of t_{cr} and t_{kz} leading to Fig. 4. Numerical estimates for the magnitude of $N^{\hat{s}\hat{s}}$ and the correlation length are discussed in the conclusions.

II. TRANSITS OF THE CRITICAL POINT: EQUILIBRIUM

In this section we will analyze the equilibrium fluctuations of \hat{s} close to critical point during a transit of the QCD critical point. Subsequently in Sect. III we will analyze the dynamics of the system to determine the corresponding non-equilibrium distribution $N^{\hat{s}\hat{s}}$.

A. Mapping the QCD equation of state onto the Ising model

To map the QCD equation of state onto the Ising model, we need to relate the temperature and chemical potential in QCD to the temperature and magnetic field of Ising system. Alternatively we may work with extensive variables and map the energy and number densities of QCD to the energy density and magnetization of the Ising model. Since the time dependence of the QCD extensive variables have already been specified in Eqs. (11) and (12), the system's trajectory in the Ising phase diagram is completely determined once this map is given.

The extensive thermodynamic variables in QCD phase diagram are denoted generically with x^a

$$x^a \equiv (e \ n), \quad (16)$$

while the corresponding thermodynamically conjugate variables are denoted with capital letters $X_a = -\partial s / \partial x^a$

$$X_a = (-\beta \ \hat{\mu}). \quad (17)$$

Here $\hat{\mu} = \mu/T$ and $\beta = 1/T$. Near the critical point the entropy can be written as a regular piece plus a singular piece³, $s = s_{\text{reg}} + s_{\text{sing}}$, where the regular piece is

$$s_{\text{reg}} = s_c + \beta_c \Delta e - \hat{\mu}_c \Delta n. \quad (18)$$

³ Strictly speaking it is the free energy and not the entropy which may be clearly divided into regular and singular pieces. s_{reg} and s_{sing} are determined from the corresponding free energies with the relation $s = \beta p + \beta e - \hat{\mu} n$, where e and n are derivatives of the free energy with respect to $-\beta$ and $\hat{\mu}$.

Then from Eq. (17) the singular part of the entropy density satisfies

$$\Delta X_a = -\frac{\partial s_{\text{sing}}}{\partial x^a} = (-\Delta\beta \ \Delta\hat{\mu}) , \quad (19)$$

with $\Delta\beta \equiv \beta - \beta_c$ etc, so that

$$ds_{\text{sing}}(x) = -\Delta X_a(x) dx^a . \quad (20)$$

Equilibrium fluctuations in QCD are treated as in Ref. [27]. In each subsystem of volume V which is large compared to the cube of the correlation length, the probability of a fluctuation $x^a \rightarrow x^a + \delta x^a$ is Gaussian and given by

$$P \propto e^{\Delta S_{(2)}} \quad \Delta S_{(2)} = -\frac{1}{2}V \mathcal{S}_{ab}(x) \delta x^a \delta x^b , \quad (21)$$

Here the matrix \mathcal{S}_{ab} is given by equilibrium thermodynamics

$$\mathcal{S}_{ab}(x) = \frac{\partial X_a(x)}{\partial x^b} = -\frac{\partial^2 s(x)}{\partial x^a \partial x^b} . \quad (22)$$

Finally if the $\delta x(\mathbf{r})$ is a function of space, the probability becomes a functional and takes the form

$$P[\delta x] \propto e^{\Delta S_{(2)}} , \quad \Delta S_{(2)} = -\frac{1}{2} \int d^3\mathbf{r} \mathcal{S}_{ab}(x) \delta x^a(\mathbf{r}) \delta x^b(\mathbf{r}) . \quad (23)$$

The extensive variables in the Ising model (the energy density and the magnetization) are denoted generically with x^A , distinguished from QCD case by the uppercase index:

$$x^A \equiv (\epsilon \ \psi) . \quad (24)$$

Here $\epsilon \equiv (\mathcal{E} - \mathcal{E}_c)/T_c^{\text{is}}$ is the deviation of Ising energy density from the critical one relative to the Ising critical temperature T_c^{is} , while ψ is the spin density (the order parameter). The thermodynamically conjugate variables are $X_A = -\partial s_{\text{sing}}/\partial x^A$

$$X_A = (r \ h) , \quad (25)$$

where $r = (T - T_c^{\text{is}})/T_c^{\text{is}}$ denotes the reduced temperature, and $h = H/T_c^{\text{is}}$ is the reduced magnetic field (see Appendix A). The singular part of the Ising entropy is

$$ds_{\text{sing, is}}(x) = -X_A(x) dx^A , \quad (26)$$

and the equilibrium quadratic functional reads

$$\Delta S_{(2)} = -\frac{1}{2} \int d^3\mathbf{r} \mathcal{S}_{AB}(x) \delta x^A(\mathbf{r}) \delta x^B(\mathbf{r}) . \quad (27)$$

The mapping between x^a and x^A or X_a and X_A is not universal but is analytic [26]. Therefore, in the vicinity of the critical point, ΔX_a and X_A are related through a linear transformation specified by 2-by-2 matrix \bar{M} :

$$X_A = \Delta X_b \bar{M}^b_A , \quad \bar{M}^b_A = \frac{\partial X_A}{\partial X_b} . \quad (28)$$

Similarly, the extensive variable are related with a 2-by-2 matrix M

$$x^A = M^A_b \Delta x^b, \quad M^A_b = \frac{\partial x^A}{\partial x^b}. \quad (29)$$

The matrices M and \bar{M} are inverses of each other. Indeed, the probability of a fluctuation in the extensive QCD parameters $\delta e, \delta n$ must be the same as a corresponding fluctuation in $\delta \epsilon, \delta \psi$ in the Ising system in order to have universal behavior. The decrease in entropy per volume $\Delta S_{(2)}$ due to a fluctuation must be the same in both systems:

$$\delta h \delta \psi + \delta r \delta \epsilon = \delta \hat{\mu} \delta n - \delta \beta \delta e \quad (30)$$

i.e. $\delta X_A \delta x^A = \delta X_a \delta x^a$. From eq. (30) we see that M and \bar{M} are inverse matrices of each other

$$M^B_a \bar{M}^a_C = \delta^B_C. \quad (31)$$

With this relation we also see that singular parts of the entropy differential ds_{sing} of the QCD and Ising systems agree.

Of the four parameters in the two-by-two matrix \bar{M} (or M), two of the parameters are just scale factors, while the remaining two parameters determine the directions of changing τ and h in the QCD T, μ plane. The line $h = 0$ is the coexistence line in the Ising system, and must correspond to the coexistence curve, $T_{\text{cx}}(\mu)$, in the QCD phase diagram. Thus, knowledge of $T_{\text{cx}}(\mu)$ places a constraint on the remaining two directional parameters of M , which is found by setting $dh = 0$ (i.e. constant h) in Eq. (28)

$$\frac{T'_{\text{cx}}}{1 - (\mu_c/T_c)T'_{\text{cx}}(\mu)} \left(\frac{1}{T_c} M_n^\epsilon \right) = M_e^\epsilon, \quad (32)$$

or equivalently

$$\frac{T'_{\text{cx}}}{1 - (\mu_c/T_c)T'_{\text{cx}}(\mu)} \left(\frac{1}{T_c} \bar{M}_h^\beta \right) = -\bar{M}_h^{\hat{\mu}}. \quad (33)$$

Following previous works [25], we ignore the μ dependence of $T_{\text{cx}}(\mu)$ and set $T'_{\text{cx}}(\mu) = 0$, and thus $M_e^\epsilon = 0$ and $\bar{M}_h^{\hat{\mu}} = 0$. For maximum simplicity we will also take the direction of increasing h in the Ising model to correspond with T direction of QCD by setting $M_n^\psi = -M_e^\psi \mu_c$. With these choices, the map is determined by two positive dimensionless scale factors, $(T_c M_e^\psi)$ and $-M_n^\epsilon$, leading to the definition

$$A_s \equiv (T_c M_e^\psi), \quad (34)$$

$$A_n \equiv -M_n^\epsilon. \quad (35)$$

The intensive parameters of the Ising model and QCD are related after elementary algebra

$$r = -\frac{1}{A_n} \frac{\Delta \mu}{T_c}, \quad (36)$$

$$h = \frac{1}{A_s} \frac{\Delta T}{T_c}. \quad (37)$$

In terms of the extensive parameters, this means that the QCD entropy is proportional to the order parameter

$$\epsilon = -A_n \Delta n, \quad (38)$$

$$\psi = A_s \Delta s, \quad (39)$$

where we have used $T_c \Delta s = \Delta e - \mu_c \Delta n$. Finally, as discussed more completely below, the Ising energy density and magnetization, (ϵ, ψ) , are determined up to two normalization constants, $(\mathcal{M}_0 h_0, \mathcal{M}_0)$. These constants can always be adjusted by redefining the mapping parameters, and we will conventionally choose

$$\mathcal{M}_0 h_0 \equiv n_c, \quad (40)$$

$$\mathcal{M}_0 \equiv s_c, \quad (41)$$

so that the scale factors (A_n, A_s) are of order unity. Thus, our final specification for how (ϵ, ψ) are related to $(\Delta n, \Delta s)$ reads

$$\frac{\epsilon}{\mathcal{M}_0 h_0} = -A_n \frac{\Delta n}{n_c}, \quad (42a)$$

$$\frac{\psi}{\mathcal{M}_0} = A_s \frac{\Delta s}{s_c}. \quad (42b)$$

Our conclusions will be largely independent of the precise form of the mapping between QCD and Ising model. What is important in what follows is that A_n and A_s are positive, dimensionless, and of order unity constants. Further Eq. (42) together with the time dependence of Δn and Δs given in Eq. (11) fully specify how the QCD system evolves in the Ising model plane as a function of time.

B. The QCD specific heat C_p and the speed of sound near the critical point

Given the Ising equation of state and the corresponding states in the QCD medium, we may compute how the QCD specific heats and the speed of sound are related to the Ising susceptibilities near the critical point. As we will review, the critical behavior of the speed of sound and the specific heat at constant pressure, C_p , are independent of the details of the mapping matrix M^A_b [26]. C_p determines the fluctuations in the entropy per baryon \hat{s} , and is the most rapidly divergent equilibrium susceptibility near the QCD critical point.

1. The Ising model susceptibilities

The Ising model susceptibilities determine the fluctuations in the extensive quantities x^A , and are given by the matrix

$$\mathcal{G}_{\text{is}}^{AB} = \frac{1}{V} \frac{\partial^2 \log Z_{\text{sing}}}{\partial X_A \partial X_B} \bigg|_{X_A=0} = V \langle \delta x^A \delta x^B \rangle. \quad (43)$$

The conventional names for the entries of this matrix are

$$\mathcal{G}_{\text{is}}^{11} \equiv C_H, \quad (44)$$

$$\mathcal{G}_{\text{is}}^{22} \equiv \chi_{\text{is}}, \quad (45)$$

$$\det \mathcal{G}_{\text{is}}^{AB} \equiv \chi_{\text{is}} C_M, \quad C_M = \mathcal{G}_{\text{is}}^{11} - \frac{(\mathcal{G}_{\text{is}}^{12})^2}{\mathcal{G}_{\text{is}}^{22}}, \quad (46)$$

where C_H is the specific heat at constant magnetic field, and C_M is the specific heat at constant magnetization. Straightforward algebra (see Appendix A for details) yields explicit

expressions for these quantities in terms of the commonly used R, θ parametrization – see Eq. (211) in Appendix A. As seen from the appended expressions, the Ising susceptibility χ_{is} and specific heat C_M diverge as

$$\chi_{\text{is}} \propto R^{-\gamma}, \quad \text{with } \gamma = 1.24, \quad (47)$$

$$C_M \propto R^{-\alpha}, \quad \text{with } \alpha = 0.11. \quad (48)$$

where $R \rightarrow 0$ near the critical point. From a perspective of heavy ion collisions, the critical exponent α is so small that it will probably never be observed, and we will focus on susceptibility χ_{is} .

The inverse matrix determines the corresponding fluctuations of the intensive parameters [27]

$$\mathcal{S}_{AB}^{\text{is}} \equiv (\mathcal{G}_{\text{is}}^{-1})_{AB} = \frac{1}{\chi_{\text{is}} C_M} \begin{pmatrix} \chi_{\text{is}} & -\mathcal{G}_{\text{is}}^{12} \\ -\mathcal{G}_{\text{is}}^{12} & C_H \end{pmatrix} = V \langle \delta X_A \delta X_B \rangle, \quad (49)$$

which follows from the definition, $X_A = -\partial S / \partial x^A$. We note the correlations between the extensive and intensive variables are simple

$$V \langle \delta x^A \delta X_B \rangle = \delta_B^A, \quad (50)$$

reflecting the relation, $\mathcal{S}^{\text{is}} = \mathcal{G}_{\text{is}}^{-1}$

Finally, let us discuss the wavenumber dependence of the Ising correlation functions. Near the critical point the correlation function of magnetization,

$$\langle \psi(\mathbf{k}) \psi(-\mathbf{k}') \rangle \equiv \mathcal{X}_{\text{is}}(k) (2\pi)^3 \delta^{(3)}(\mathbf{k} - \mathbf{k}'), \quad (51)$$

takes the form

$$\mathcal{X}_{\text{is}}(k) = \chi_{\text{is}} K_{\chi}(k\xi), \quad (52)$$

where $K_{\chi}(k\xi)$ is a static universal function with unit normalization⁴, $K_{\chi}(0) = 1$. K_{χ} has been studied extensively [31], and for $k \gg \xi^{-1}$ takes the asymptotic form

$$\chi_{\text{is}} K_{\chi}(k\xi) = \frac{C_{\infty}}{k^{2-\eta}}, \quad (53)$$

where $\eta \simeq 0.036$ is the critical exponent, and the constant C_{∞} is independent of ξ . In coordinate space the correlation function behaves as $\sim 1/r^{1+\eta}$ at small r . This singular behaviour is ultimately cutoff for $r \sim \ell_0$. We will use the simple Ornstein-Zernicke form [26]

$$K_{\chi}(k\xi) = \frac{1}{1 + (k\xi)^{2-\eta}}, \quad (54)$$

which has the correct limits for $k \ll \xi^{-1}$, and $k \gg \xi^{-1}$.

⁴ In principle, K_{χ} will be different inside and outside coexistence regime [30]. While including such dependence is straightforward, we will neglect this refinement in the current study.

2. The QCD susceptibilities

The corresponding QCD susceptibility matrices are

$$\mathcal{G}^{ab} = \frac{1}{V} \frac{\partial^2 \log Z_{\text{sing}}}{\partial X_a \partial X_b}, \quad \mathcal{S}_{ab} \equiv (\mathcal{G}^{ab})^{-1}, \quad (55)$$

which determine the QCD fluctuations $\langle \delta x^a \delta x^b \rangle$, and $\langle \delta X_a \delta X_b \rangle$ respectively. The matrix \mathcal{G}^{ab} determines the speed of sound c_s^2 and the fluctuations in the entropy per baryon as we review below.

To write down the formulas relating the speed of sound to \mathcal{G}^{ab} , we define derivatives of the pressure

$$p^a \equiv \frac{\partial p}{\partial X_a}, \quad (p^e, p^n) = \left(-\frac{\partial p}{\partial \beta}, \frac{\partial p}{\partial \hat{\mu}} \right) = \left(\frac{w}{\beta}, \frac{n}{\beta} \right), \quad (56)$$

and then the speed of sound, $c_s^2 = (\partial p / \partial e)_{n/s}$, is given by

$$c_s^2 = \left(\frac{\partial p}{\partial e} \right)_n + \frac{n}{w} \left(\frac{\partial p}{\partial n} \right)_e, \quad (57a)$$

$$= \frac{\beta}{w} p^a \mathcal{S}_{ab} p^b. \quad (57b)$$

As usual, $w \equiv e + p$ is the enthalpy density. From this expression we see that fluctuations in the pressure $\delta p = p^a \delta X_a$ determine the speed of sound

$$V \langle \delta p^2 \rangle = p^a \mathcal{S}_{ab} p^b = \frac{w c_s^2}{\beta}. \quad (58)$$

The fluctuations in the entropy per baryon will play a central role in what follows, and thus we define

$$\delta \hat{s} \equiv n \delta \left(\frac{s}{n} \right) = \delta s - \frac{s}{n} \delta n. \quad (59)$$

The fluctuations in \hat{s} can be written in terms of δe and δn

$$T \delta \hat{s} = \delta e - \frac{w}{n} \delta n, \quad (60)$$

and are uncorrelated with the fluctuations in the pressure

$$\langle \delta p \delta \hat{s} \rangle = 0, \quad (61)$$

which can be derived from Eq. (50) and Eq. (56). A more complete discussion of this and the thermodynamic relations in the rest of this section is given in Refs. [26, 27]. The fluctuations in \hat{s} are determined by the specific heat at constant pressure, $C_p \equiv nT \left(\frac{\partial(s/n)}{\partial T} \right)_p$, via

$$N^{\hat{s}\hat{s}} \equiv V \langle (\delta \hat{s})^2 \rangle = V \left\langle \left(\delta s - \frac{s}{n} \delta n \right)^2 \right\rangle = C_p. \quad (62)$$

Straightforward analysis shows that C_p is related to determinant of the susceptibility matrix

$$\left(\frac{nT}{w} \right)^2 C_p = \frac{\beta c_s^2}{w} \det \mathcal{G}^{ab}. \quad (63)$$

The specific heat at constant pressure is also related to the specific heat at constant volume $C_V \equiv T(\partial s/\partial T)_n$ through the familiar relation

$$\left(\frac{nT}{w}\right)^2 C_p = T \frac{\partial n}{\partial \mu} \left(\frac{TC_V c_s^2}{w}\right). \quad (64)$$

In the low density limit, $n \rightarrow 0$, the final factor on the r.h.s. approaches unity, $(TC_V c_s^2/w) \rightarrow 1$. Eq. (64) leads to an important relation, Eq. (121) below, between the baryon number diffusion coefficient and the diffusion coefficient of \hat{s} .

In practice, both theoretically and experimentally, it is easier to work with the correlation function of \hat{s} rather than fluctuations of \hat{s} in a finite volume V

$$N^{\hat{s}\hat{s}}(t, \mathbf{k}) \equiv \int d^3x e^{i\mathbf{k}\cdot(\mathbf{x}-\mathbf{y})} \langle \delta\hat{s}(t, \mathbf{x}) \delta\hat{s}(t, \mathbf{y}) \rangle. \quad (65)$$

In equilibrium, Eq. (62) predicts that $N^{\hat{s}\hat{s}}(t, \mathbf{k})$ approaches C_p as $\mathbf{k} \rightarrow 0$.

3. QCD fluctuations near the critical point

We have now specified how the speed of sound and specific heats are related to the QCD susceptibility matrix \mathcal{G}^{ab} . The QCD susceptibilities are related to the corresponding Ising quantities with the mapping matrices of Sect. II A.

$$\mathcal{G}^{ab} = \bar{M}_A^a \bar{M}_B^b \mathcal{G}_{\text{is}}^{AB}. \quad (66)$$

As we will now review, near the critical point the speed of sound, c_s^2 , approaches zero as $C_M^{-1} \propto R^\alpha$, while the specific heat, C_p , diverges as $\chi_{\text{is}} \propto R^{-\gamma}$ [26]. This is independent of the details of the mapping matrix M_A^b . From a practical perspective this means that the softening of the equation of state near the critical point will probably be too small to observe (since α is small), and the experimental heavy ion program should focus on the fluctuations in s/n which reflects the diverging value of the specific heat $C_p \propto \chi_{\text{is}}$.

To review how the speed of sound behaves near the Ising critical point, we first note that by inserting unity of the form $\bar{M}_B^a M_c^B = \delta_c^a$ into Eq. (58), we can express the speed of sound near the critical point as

$$c_s^2 = \frac{\beta}{w} p^A S_{AB} p^B \simeq \frac{\beta}{w} \left(\frac{\partial p}{\partial r}\right)^2 \frac{1}{C_M}, \quad (67)$$

where we define $p^A = (\partial p/\partial X_A)$ and thus $(\partial p/\partial r)_h = M_n^\epsilon p^n + M_e^\epsilon p^e$, is derivative of the QCD pressure in the direction of reduced Ising temperature. We note that $(\partial p/\partial r)$ remains finite near the critical point. In approximating Eq. (67), we recognized that near the critical point χ_{is} is strongly divergent, and thus the rr component in $p^A S_{AB} p^B$ dominates the sum. This shows (as claimed) that the speed of sound approaches zero like the Ising specific heat C_M^{-1} , i.e. as R^α . In the case of the simple mapping described in Sect. II A we have

$$c_s^2 = \frac{\beta}{w} \frac{(T_c n_c A_n)^2}{C_M}. \quad (68)$$

In the rest of this paper we will focus on the specific heat C_p which exhibits a much more dramatic behavior, diverging as $R^{-\gamma}$ near the critical point.

The behavior of C_p near the critical point is determined by the determinant in Eq. (63) and the relation between the determinants of the QCD and Ising systems

$$\det \mathcal{G}^{ab} = (\det \bar{M})^2 \det \mathcal{G}_{\text{is}}^{AB} \quad (69)$$

Thus since $\det \mathcal{G}_{\text{is}}^{AB} = \chi_{\text{is}} C_M$, we find with Eqs. (63) and (67) that

$$C_p = \frac{\left(\frac{1}{T_c n_c} \frac{\partial p}{\partial r} \right)^2}{(T_c \det M)^2} \chi_{\text{is}}. \quad (70)$$

The factors $(T_c \det M)$ and $(\partial p / \partial r) / n_c T_c$ are both dimensionless and of order unity. Thus, independently of the details between the QCD and Ising variables, the specific heat C_p is proportional to the Ising susceptibility χ_{is} and diverges as $R^{-\gamma}$. For the simple mapping of Sect. II A the specific heat takes the particularly simple form

$$C_p = \frac{\chi_{\text{is}}}{A_s^2}, \quad (71)$$

which we will assume in what follows.

Finally, later we will study the correlation function $N^{\hat{s}\hat{s}}(t, \mathbf{k})$ as a function of \mathbf{k} . In equilibrium, this will take the form

$$N_0^{\hat{s}\hat{s}}(t, \mathbf{k}) = \frac{\chi_{\text{is}}}{A_s^2} \frac{1}{1 + (k\xi)^{2-\eta}}, \quad (72)$$

where we have adopted for simplicity Ornstein-Zernicke form, which has the properties discussed in Sect. II B 1.

At this point we need to determine how the parameters $\chi_{\text{is}}(t)$ and $\xi(t)$ depend on time when Δn and Δs follow the adiabatic trajectory parametrized by Eq. (11). We will turn to this task in the next section.

C. The timescale for the scaling regime during a transit of the QCD critical point

We have now specified how the extensive Ising variables (ϵ, ψ) are determined by the QCD quantities $(\Delta n, \Delta s)$ with Eq. (42). We also have specified how the extensive QCD quantities depend on time in Eq. (11). Finally, the Ising equation of state determines the time dependence of the corresponding susceptibilities and correlation lengths, from the time dependent extensive Ising variables. In this section we will show how the scaling form of the Ising equation of state leads to a characteristic scaling form in time for these quantities.

Outside of the coexistence region, the scaling of the Ising equation of state implies the following scaling forms for the extensive variables (ϵ, ψ) as a function of (r, h)

$$\epsilon = \mathcal{M}_0 h_0 |r|^{1-\alpha} f_\epsilon(z), \quad (73a)$$

$$\psi = \mathcal{M}_0 |r|^\beta f_\psi(z), \quad (73b)$$

Here $(\mathcal{M}_0 h_0, \mathcal{M}_0) \equiv (n_c, s_c)$ are two (conventional) constants described above, and below $f_X(z)$ denotes a generic universal scaling function of the variable $z \propto r/|h|^{1/\beta\delta}$ (see Eq. (200) in Appendix A for a complete definition of z .) All susceptibilities and correlation lengths

take this generic form, and no additional constants need to be introduced. In practice, given (ϵ, ψ) we numerically determine (R, θ) from the Ising parametrization described in Appendix A, and then evaluate all other thermodynamic functions.

As $z \rightarrow z_0 \equiv -\infty$, the system approaches the coexistence region, and $f_\epsilon(z)$ and $f_\psi(z)$ approach -1 and 1 by convention⁵. Inside the coexistence region the energy density is related to the temperature by

$$\epsilon = -\mathcal{M}_0 h_0 |r|^{1-\alpha}, \quad (74)$$

and the magnetization lies in the range $(-\psi_0, \psi_0)$ where

$$\psi_0 = \mathcal{M}_0 |r|^\beta. \quad (75)$$

These expressions for the extensive quantities in terms of the intensive ones may be inverted. We define a new scaling variable based on extensive variables

$$u \equiv \frac{\epsilon}{\mathcal{M}_0 h_0} \left(\frac{\mathcal{M}_0}{|\psi|} \right)^b, \quad (76)$$

where $b = (1 - \alpha)/\beta \simeq 2.7$, and then outside the coexistence region

$$r = \left(\frac{|\epsilon|}{\mathcal{M}_0 h_0} \right)^a f_r(u), \quad (77)$$

$$z = f_z(u), \quad (78)$$

with $a = 1/(1 - \alpha) \simeq 1.12$. The system is in the coexistence region for $u < -1$.

The advantage of a scaling variable based on extensive quantities is that the extensive quantities depend on time in a simple way. Indeed, the scaling variable u is approximately linear in time

$$u = \frac{A_n t / \tau_Q}{(A_s (\Delta_s - t / \tau_Q))^b} \simeq \frac{A_n}{A_s^b} \frac{t}{\tau_Q \Delta_s^b}. \quad (79)$$

In the last step, we recognized that in order to see the detailed scaling structure in the equation of state (which is parametrized by $f_r(u)$ in (77)), we must have $|u| \sim |z| \sim |\theta| \sim 1$. For $|u| \sim 1$, $|t / \tau_Q| \sim \Delta_s^b$ and is small compared Δ_s in this regime. From the last equality of Eq. (79), the system crosses the detailed scaling regime over a time period of order

$$t_{\text{cr}} \sim \tau_Q \Delta_s^b. \quad (80)$$

Parametrically outside of this time window the scaling functions such as $f_r(u)$ may be treated as constants. Inside of this time window the QCD parameters are of order

$$\frac{\Delta_s}{s_c} \sim \Delta_s, \quad \frac{\Delta_n}{n_c} \sim \Delta_s^b. \quad (81)$$

Accordingly, in Fig. 1(c) we have rescaled the x and y axis by Δ_s^b and Δ_s , which flattens the 45° trajectory lines in Fig. 1(b). It is only in this regime that the detailed scaling structure of the Ising equation of state (as recorded by the (R, θ) parametrization) is really necessary.

⁵ A handy Mathematica notebook which evaluates all universal Ising thermodynamic variables and correlation lengths is made available as part of this work.

To simplify notation we absorb the mapping constants into the definition of the parameters defining

$$\bar{\tau}_Q \equiv \frac{\tau_Q}{A_n}, \quad (82)$$

$$\bar{\Delta}_s \equiv A_s \Delta_s. \quad (83)$$

The crossing time is defined as the time when the system leaves the coexistence region (see Fig. 1(c))

$$t_{\text{cr}} \equiv -\bar{\tau}_Q \bar{\Delta}_s^b, \quad \text{with} \quad u = \frac{t}{|t_{\text{cr}}|}, \quad (84)$$

so $u = -1$ corresponds to $t = t_{\text{cr}}$. The Ising energy and order parameter have a simple time dependence

$$\epsilon = \mathcal{M}_0 h_0 \frac{t}{\bar{\tau}_Q}, \quad \psi = \mathcal{M}_0 \bar{\Delta}_s. \quad (85)$$

The scaling of the Ising susceptibility and other thermodynamic quantities with ϵ and u imply a specific scaling in time. For instance, using the Ising parametrization in Appendix A, the susceptibility behaves as

$$\chi_{\text{is}} = \chi_0 \left(\frac{|\epsilon|}{\mathcal{M}_0 h_0} \right)^{-a\gamma} f_\chi(u), \quad (86)$$

where

$$\chi_0 \equiv 0.365 \frac{s_c^2}{n_c}. \quad (87)$$

is the typical size of C_p away from the critical point, and we recall that $s_c^2/n_c = \mathcal{M}_0/h_0$. The scaling function is continuous and takes the form

$$f_\chi(u) = \begin{cases} 1 & u < -1 \\ f_\chi(u) & u > -1 \end{cases}, \quad (88)$$

with limiting values

$$f_\chi(-1) = 1, \quad f_\chi(u) \xrightarrow{u \rightarrow \infty} f_\chi^+ \equiv 1.954. \quad (89)$$

The combination $|u|^{-a\gamma} f_\chi(u)$ is regular and decreasing for $u > -1$. Thus, the equilibrium susceptibility as a function of time takes the following form

$$\chi_{\text{is}} = \chi_0 \left(\frac{|t|}{\bar{\tau}_Q} \right)^{-a\gamma} f_\chi \left(\frac{t}{|t_{\text{cr}}|} \right), \quad (90a)$$

which can be written as function $t/|t_{\text{cr}}|$ using Eq. (84)

$$\chi_{\text{is}} = \chi_0 (\bar{\Delta}_s)^{-\gamma/\beta} \left| \frac{t}{t_{\text{cr}}} \right|^{-a\gamma} f_\chi \left(\frac{t}{|t_{\text{cr}}|} \right). \quad (90b)$$

Eq. 90b is plotted in Fig. 2(a). To evaluate $|u|^{-a\gamma} f_\chi(u)$ in practice, we determine the (R, θ) associated with (ϵ, u) numerically – see Appendix A.

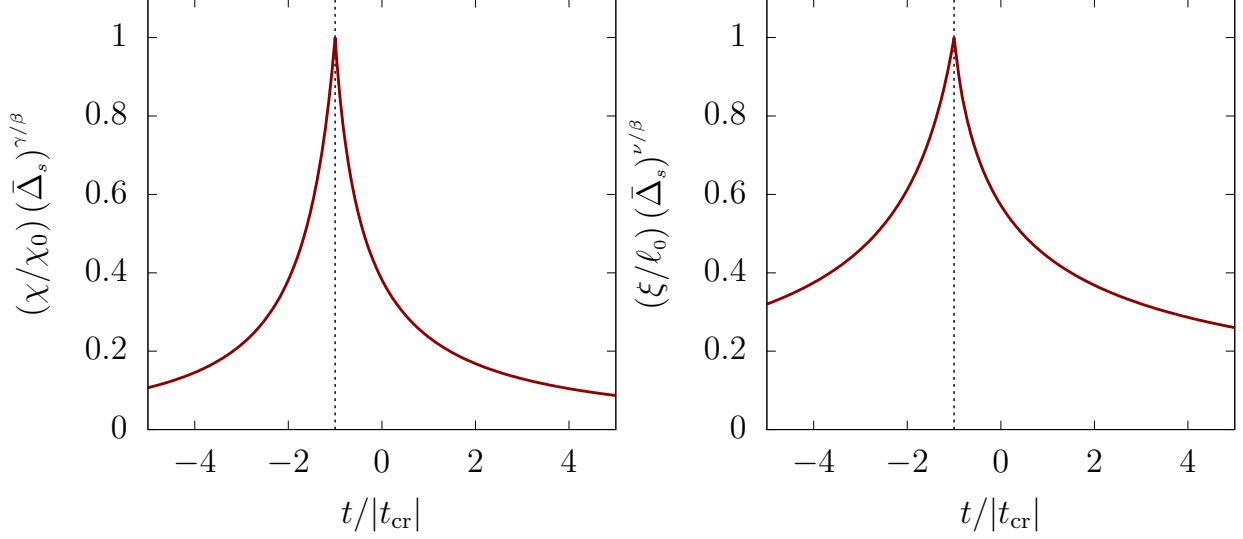


FIG. 2. The Ising susceptibility and correlation length as a function of time during a transit of the QCD critical point along an adiabatic trajectory characterized by $\bar{\Delta}_s$. The time axis has been rescaled by $t_{\text{cr}} \sim \tau_Q \Delta_s^b$, see Eq. (84). The y axes have been rescaled by an appropriate power of $\bar{\Delta}_s$ so that the curve is independent of $\bar{\Delta}_s$.

The correlation length follows a similar pattern. The equilibrium correlation length in the Ising model takes the scaling form (see Appendix A)

$$\xi(t) = \ell_o \left(\frac{|\epsilon|}{\mathcal{M}_0 h_0} \right)^{-a\nu} f_\xi(u), \quad (91)$$

where

$$\ell_0 \equiv 0.365 n_c^{-1/3}, \quad (92)$$

is of order the inter-particle spacing, and we recall that $\mathcal{M}_0 h_0 = n_c$. The limiting values of the analogous scaling function $f_\xi(u)$ are

$$f_\xi(-1) = 1, \quad f_\xi(u) \xrightarrow{u \rightarrow \infty} f_\xi^+ \equiv 1.222, \quad (93a)$$

and $|u|^{-a\nu} f_\xi(u)$ is regular and decreasing for $u > -1$. The equilibrium correlation length as a function of time takes form

$$\xi(t) = \ell_0 \left(\frac{|t|}{\bar{\tau}_Q} \right)^{-a\nu} f_\xi \left(\frac{t}{|t_{\text{cr}}|} \right), \quad (94a)$$

or after using the definition of t_{cr} (Eq. (84))

$$\xi(t) = \ell_0 (\bar{\Delta}_s)^{-\nu/\beta} \left| \frac{t}{t_{\text{cr}}} \right|^{-a\nu} f_\xi \left(\frac{t}{|t_{\text{cr}}|} \right). \quad (94b)$$

Eq. 94b is plotted in Fig. 2(b). To evaluate $|u|^{-a\nu} f_\xi(u)$ in practice we use the numerical data on the Ising model from Engels, Fromme and Seniuch [32] – see Appendix A.

D. Summary of the equilibrium expectation

To conclude this section let us collect and review the equilibrium formulas. $N^{\hat{s}\hat{s}}(t, \mathbf{k})$ in equilibrium takes the approximate form, from Eqs. (71) and (72),

$$N_0^{\hat{s}\hat{s}}(t, \mathbf{k}) = \frac{1}{A_s^2} \frac{\chi_{\text{is}}(t)}{1 + (k\xi(t))^{2-\eta}}. \quad (95)$$

where A_s is a constant determined by the mapping between QCD and the Ising model. The specific heat and equilibrium correlation length are universal functions of time as shown in Fig. 2, and the timescale for their evolution is set by $t_{\text{cr}} \sim \tau_Q \Delta_s^b$. In the next section we will describe how the system evolves according to stochastic hydrodynamics, and tries to approach this time dependent equilibrium expectation.

III. TRANSITS OF THE CRITICAL POINT: DYNAMICS

The primary purpose of this work is to discuss the fluctuations of thermodynamic variables (e.g. e, n) for a system transiting close to the QCD critical point. Specifically, we will focus on the time evolution of the correlation functions of the thermodynamic variables, which quantify the fluctuations with a specific wave number k . In the previous section, we have analyzed the equilibrium behavior of these correlations, and now we will study their dynamical evolution.

We first determine this evolution in the hydrodynamic regime, $k \ll \xi^{-1}$. To this end, we start from fluctuating hydrodynamics, and derive a set of relaxation equations for the correlations, which we refer to as the hydro-kinetic equations [11]. In the previous section, we showed that critical fluctuations are more enhanced in the \hat{s} mode than in any other combination of thermodynamic variables. When we apply the hydro-kinetic equations (Eq. (122) below) to a system near a critical point, we find that the equilibration of the \hat{s} correlator $N^{\hat{s}\hat{s}}$ is independent of the other hydrodynamic modes, allowing us to focus on $N^{\hat{s}\hat{s}}$.

The description of $N^{\hat{s}\hat{s}}$ near a critical point, even in equilibrium, involves an additional length scale. As we have seen in Eq. (95), the behavior of $N^{\hat{s}\hat{s}}$ in equilibrium exhibits a non-trivial dependence on the wavenumber k , and such dependence is characterized by the correlation length ξ . To model the off-equilibrium evolution of $N^{\hat{s}\hat{s}}$ in the scaling region, we need to extend the hydro-kinetic equations to larger k , $\xi^{-1} \lesssim k \ll \ell_0^{-1}$. This is done schematically in Sect. III B – see Eq. (129). It should be made clear that Eq. (129) is simply a rough model we will use to describe the dynamics of $N^{\hat{s}\hat{s}}$ in the scaling regime, and we defer a systematic treatment to future work. In Sect. III C, we estimate the characteristic time and length scales of $N^{\hat{s}\hat{s}}$. Finally, we evaluate $N^{\hat{s}\hat{s}}$ numerically by solving Eq. (129) numerically to determine the time evolution fluctuations during a transit of the critical point.

A. The evolution of fluctuations for a fluid with finite baryon density

1. The derivation of hydro-kinetic equations

We begin by considering the fluctuations around a uniform static fluid background of the extensive thermodynamic variables $e(t, \mathbf{x}) = e + \delta e(t, \mathbf{x})$, $n(t, \mathbf{x}) = n + \delta n(t, \mathbf{x})$, and momentum $\vec{g}(t, \mathbf{x}) \equiv w\vec{u}(t, \mathbf{x})$, where $\vec{u}(t, \mathbf{x})$ denotes the fluid velocity. In k -space, the

fluctuations of longitudinal momentum $g \equiv \vec{g} \cdot \hat{k}$ will mix with $\delta e, \delta n$ at finite density, and we will denote them collectively as⁶:

$$\delta x^{\bar{a}} \equiv (\delta e, \delta n, g) . \quad (96)$$

Transverse components of the momentum, $\vec{g}_T \cdot \vec{k} = 0$, decouple from $\delta x^{\bar{a}}$ modes in the linear regime (see Eq. (100) below).

We are interested in the equal-time correlation function $N^{\bar{a}\bar{b}}(t, \mathbf{k})$ in k -space:

$$\langle \delta x^{\bar{a}}(t, \mathbf{k}) \delta x^{\bar{b}}(t, -\mathbf{k}') \rangle \equiv (2\pi)^3 \delta^{(3)}(\mathbf{k} - \mathbf{k}') N^{\bar{a}\bar{b}}(t, \mathbf{k}) , \quad (97)$$

The equilibrium values of $N^{\bar{a}\bar{b}}$, namely $N_0^{\bar{a}\bar{b}}$, are given by the susceptibility matrix:

$$N_0^{\bar{a}\bar{b}} = (\mathcal{S}_{\bar{a}\bar{b}})^{-1} , \quad (98)$$

where

$$\mathcal{S}_{\bar{a}\bar{b}} = \begin{pmatrix} \mathcal{S}_{ee} & \mathcal{S}_{en} & 0 \\ \mathcal{S}_{ne} & \mathcal{S}_{nn} & 0 \\ 0 & 0 & \frac{\beta}{w} \end{pmatrix} , \quad (99)$$

and where $\mathcal{S}_{ee}, \mathcal{S}_{en}, \mathcal{S}_{nn}$ are defined in Eq. (22).

In order to derive a relaxation equation for $N^{\bar{a}\bar{b}}(t, \mathbf{k})$, we consider the linearized stochastic hydrodynamic equations in the k -space:

$$\frac{\partial}{\partial t} \delta e(t, \mathbf{k}) = -i\vec{k} \cdot \vec{g} , \quad (100a)$$

$$\frac{\partial}{\partial t} \delta n(t, \mathbf{k}) = -\frac{n}{w} i\vec{k} \cdot \vec{g} - \lambda_B T k^2 \delta \hat{\mu} - \xi_n , \quad (100b)$$

$$\frac{\partial}{\partial t} \vec{g}(t, \mathbf{k}) = -i\vec{k} \delta p - \frac{\eta k^2}{w} \vec{g} - \frac{\zeta + \frac{1}{3}\eta}{w} \vec{k} (\vec{k} \cdot \vec{g}) - \vec{\xi} . \quad (100c)$$

The noise terms are introduced above to describe dynamics of hydrodynamic fluctuations⁷, and the noise correlations are constrained by the fluctuation-dissipation theorem (see for example Ref. [27]):

$$\langle \xi^i(t, \mathbf{k}) \xi^j(t', -\mathbf{k}') \rangle = 2T \left[\eta k^2 \delta^{ij} + \left(\zeta + \frac{1}{3}\eta \right) k^i k^j \right] (2\pi)^3 \delta^{(3)}(\mathbf{k} - \mathbf{k}') \delta(t - t') , \quad (101a)$$

$$\langle \xi_n(t, \mathbf{k}) \xi_n(t', -\mathbf{k}') \rangle = 2T \lambda_B k^2 (2\pi)^3 \delta^{(3)}(\mathbf{k} - \mathbf{k}') \delta(t - t') , \quad (101b)$$

$$\langle \xi^i(t, \mathbf{k}) \xi_n(t', -\mathbf{k}') \rangle = 0 . \quad (101c)$$

As usual, shear viscosity, bulk viscosity and baryon conductivity are denoted by η, ζ, λ_B respectively.

⁶ The bar in $x^{\bar{a}}$ and $X^{\bar{a}}$ indicate that the longitudinal momentum and velocity are appended to the set x^a and X^a defined in Sect. II A

⁷ We use the Landau fluid frame throughout, and therefore the noise is absent in the first equation of Eq. (100).

From the hydrodynamic equation (100), we write the equation for $x^{\bar{a}}$ in a compact fashion:

$$\begin{aligned}\frac{\partial}{\partial t}\delta x^{\bar{a}}(t, \mathbf{k}) &= -ik\mathcal{L}^{\bar{a}\bar{b}}\delta X_{\bar{b}} + k^2\Lambda^{\bar{a}\bar{b}}\delta X_{\bar{b}} + \xi^{\bar{a}}, \\ &= -ikL^{\bar{a}}_{\bar{b}}\delta x^{\bar{b}} + k^2\mathcal{D}^{\bar{a}}_{\bar{b}}\delta x^{\bar{b}} + \xi^{\bar{a}},\end{aligned}\quad (102a)$$

with noise correlator

$$\langle \xi^{\bar{a}}(t, \mathbf{k}) \xi^{\bar{b}}(t', -\mathbf{k}') \rangle = 2k^2\Lambda^{\bar{a}\bar{b}}(2\pi)^3\delta^{(3)}(\mathbf{k} - \mathbf{k}')\delta(t - t'). \quad (102b)$$

Here the matrices are

$$\mathcal{L}^{\bar{a}\bar{b}} = \begin{pmatrix} 0 & 0 & p^e \\ 0 & 0 & p^n \\ p^e & p^n & 0 \end{pmatrix}, \quad \Lambda^{\bar{a}\bar{b}} = T \begin{pmatrix} 0 & 0 & 0 \\ 0 & \lambda_B & 0 \\ 0 & 0 & \zeta + \frac{4}{3}\eta \end{pmatrix}, \quad (103)$$

with $(p^e, p^n) = (w/\beta, n/\beta)$ defined in Eq. (56). Generalizing the discussion in Sect. II A, we have introduced conjugate variables through the relation $\delta X_{\bar{a}} = \mathcal{S}_{\bar{a}\bar{b}}\delta x^{\bar{b}}$

$$X_{\bar{a}} \equiv \left(-\beta, \hat{\mu}, \frac{\beta g}{w} \right). \quad (104)$$

In the second line of Eq. (102), we have further defined:

$$L^{\bar{a}}_{\bar{c}} \equiv \mathcal{L}^{\bar{a}\bar{b}}\mathcal{S}_{\bar{b}\bar{c}}, \quad (105)$$

$$\mathcal{D}^{\bar{a}}_{\bar{c}} \equiv \Lambda^{\bar{a}\bar{b}}\mathcal{S}_{\bar{b}\bar{c}}. \quad (106)$$

By carefully averaging out the noise, we obtain the following equation for $N^{\bar{a}\bar{b}}$ from Eq. (102)

$$\begin{aligned}\frac{\partial}{\partial t}N(t, \mathbf{k}) &= -ik(L \cdot N - N \cdot L^T) - k^2(\mathcal{D} \cdot N + N \cdot \mathcal{D}^T) + 2k^2\Lambda \\ &= -ik(L \cdot N - N \cdot L^T) - k^2(\mathcal{D} \cdot N + N \cdot \mathcal{D}^T) + k^2(\mathcal{D} \cdot N_0 + N_0 \cdot \mathcal{D}^T),\end{aligned}\quad (107)$$

where in the second line of Eq. (107), we have used the relation (106) and $N_0 = \mathcal{S}^{-1}$. The last term on the R.H.S. of Eq. (107) arises from the noise $\xi^{\bar{a}}$ and acts as a source. The correlations will propagate and dissipate, as described by the first and second terms on the R.H.S. of Eq. (107) respectively. When $N = N_0$, the propagation term vanishes, i.e. $L \cdot N_0 - N_0 \cdot L = 0$, and the last two terms on the R.H.S of Eq. (107) balance with each other. Therefore, N_0 is a static solution to Eq. (107) as it should be.

Following Ref. [11] and for later convenience, we will consider the fluctuations in $\delta x^{(\alpha)}$, which is given by a specific linear combination of $\delta x^{\bar{a}}$, namely $\delta x^{(\alpha)} \equiv \delta x^{\bar{a}}e_{\bar{a}}^{(\alpha)}$. Here $e_{\bar{a}}^{(\alpha)}$ is defined as the left eigenvectors for the non-hermitian matrix L :

$$\sum_{\bar{a}} e_{\bar{a}}^{(\alpha)} L^{\bar{a}}_{\bar{b}} = \lambda^{\alpha} e_{\bar{b}}^{(\alpha)}, \quad \sum_{\bar{b}} L^{\bar{a}}_{\bar{b}} e_{(\alpha)}^{\bar{b}} = \lambda^{\alpha} e_{(\alpha)}^{\bar{a}}, \quad (108)$$

where λ^{α} are corresponding eigenvalues, and where we have also introduced right eigenvectors $e_{(\alpha)}^{\bar{a}}$. Here $e_{(\alpha)}^{\bar{a}}$ and $e_{\bar{a}}^{(\alpha)}$ satisfy the orthogonality relations:

$$\sum_{\bar{a}} e_{\bar{a}}^{(\alpha)} e_{(\beta)}^{\bar{a}} = \delta^{\alpha}_{\beta}, \quad \sum_{\alpha} e_{(\alpha)}^{\bar{a}} e_{\bar{b}}^{(\alpha)} = \delta^{\bar{a}}_{\bar{b}}. \quad (109)$$

Consequently, L^α_β is diagonalized as

$$L^\alpha_\beta \equiv e^{(\alpha)}_{\bar{a}} L_{\bar{b}} e^{(\beta)}_{\bar{b}} = \lambda^\alpha \delta^\alpha_\beta. \quad (110)$$

We denote the three eigen-modes by $\alpha = +, -, \hat{s}$ for reasons which will become obvious shortly. In what follows, we will consider the correlation functions of those modes:

$$\langle \delta x^\alpha(t, \mathbf{k}) \delta x^\beta(t, -\mathbf{k}') \rangle \equiv (2\pi)^3 \delta^{(3)}(\mathbf{k} - \mathbf{k}') N^{\alpha\beta}(t, \mathbf{k}). \quad (111)$$

To better understand the physical meaning of $\delta x^{(\alpha)}$, we write down the eigenvalues

$$\lambda^\pm = \pm c_s, \quad \lambda^{\hat{s}} = 0, \quad (112)$$

and specific form of the eigenvectors:

$$e^{(\pm)} = \frac{1}{\sqrt{2}} \begin{pmatrix} 1 \\ \frac{n}{w} \\ \pm c_s \end{pmatrix}, \quad e^{(\hat{s})} = \frac{nT}{c_s^2 w} \begin{pmatrix} \frac{\partial p}{\partial n} \\ -\frac{\partial p}{\partial e} \\ 0 \end{pmatrix}, \quad (113a)$$

$$e^{(\pm)} = \frac{1}{\sqrt{2}c_s^2} \begin{pmatrix} \frac{\partial p}{\partial e} \\ \frac{\partial p}{\partial n} \\ \pm c_s \end{pmatrix}, \quad e^{(\hat{s})} = \left(\frac{1}{T}, -\frac{w}{nT}, 0 \right). \quad (113b)$$

Consequently,

$$\delta x^{(\pm)} = \frac{1}{\sqrt{2}c_s^2} (\delta p \pm c_s g), \quad \delta x^{(\hat{s})} = \delta \hat{s}. \quad (114)$$

It should be clear now that those two modes with eigenvalues $\pm c_s$ correspond to two propagating sound modes, and the mode with zero eigenvalue is identical to the \hat{s} mode. To find the equilibrium variances of these fluctuations we evaluate $N_0^{\alpha\beta} = e^{(\alpha)}_{\bar{a}} N_0^{\bar{a}\bar{b}} e^{(\beta)}_{\bar{b}}$ and find the non-zero components

$$N_0^{++} = N_0^{--} = \frac{w}{\beta c_s^2}, \quad N_0^{\hat{s}\hat{s}} = C_p, \quad (115)$$

which should be compared with Eqs. (58), (61), and (62) of the previous section. Note that the fluctuations of \hat{s} are uncorrelated with the pressure fluctuations $\delta x^{(\pm)}$.

We can now determine the dynamical equation for $N^{\alpha\beta}$ by expressing Eq. (107) in the eigen-basis of L , after defining the matrix elements

$$\mathcal{D}^\alpha_\beta \equiv e^{(\alpha)}_{\bar{a}} \mathcal{D}_{\bar{b}} e^{(\beta)}_{\bar{b}}, \quad (116)$$

In the eigen-basis of L the diagonal components $(L \cdot N - N \cdot L)^{\alpha\alpha}$ vanish, and $N^{\alpha\alpha}$ will dissipate but will not oscillate as a function of time. By contrast, the off-diagonal components of $(L \cdot N - N \cdot L)^{\alpha\beta}$ are found to be proportional to c_s , and rotate rapidly. This observation allows us to neglect off-diagonal components of $N^{\alpha\beta}$ and to focus on the evolution of $N^{\alpha\alpha}$. This kinetic (or WKB) approximation to the linearized hydrodynamic wave equations is described in greater detail in Refs. [11, 33]. Taking the diagonal components of Eq. (107), we find:

$$\partial_t N^{\alpha\alpha}(t, \mathbf{k}) = -2D_\alpha k^2 (N^{\alpha\alpha}(t, k) - N_0^{\alpha\alpha}), \quad (117)$$

where we have used the fact that $N_0^{\alpha\beta}$ is a diagonal matrix. The diffusion coefficients $D_\alpha \equiv \mathcal{D}^\alpha_\alpha$ can be found by explicit calculation:

$$D_\pm = \frac{1}{2} \left[\frac{\lambda_B}{w c_s^2} \left(\frac{\partial p}{\partial n} \right)_e^2 + \frac{1}{w} \left(\zeta + \frac{4}{3} \eta \right) \right],$$

$$D_{\hat{s}} = \frac{T \lambda_B}{(nT/w)^2 C_p}. \quad (118)$$

It is useful to define the thermal conductivity λ_T with a Franz-Wiedemann type relation

$$\lambda_T \equiv \frac{T \lambda_B}{(nT/w)^2}, \quad (119)$$

so that

$$D_{\hat{s}} = \frac{\lambda_T}{C_p}. \quad (120)$$

Eq. (117) extends the hydro-kinetic equations of a charge-neutral fluid [11] to finite baryon density (see also Refs. [18, 28]). The equilibration rate of $N^{\hat{s}\hat{s}}$ is controlled by diffusion coefficient $D_{\hat{s}}$ in Eq. (120). Using the thermodynamic relation, Eq. (64), and the definition of the baryon number diffusion coefficient, $D_B = \lambda_B/(\partial n/\partial \mu)_T$, we can relate $D_{\hat{s}}$ to D_B

$$D_{\hat{s}} = D_B \left(\frac{w}{T C_V c_s^2} \right). \quad (121)$$

The coefficient in parenthesis approaches unity as $n \rightarrow 0$, and is never far from unity for the baryon densities explored at RHIC. Thus, $D_{\hat{s}}$ can be estimated from the baryon diffusion coefficient, D_B .

So far, we have derived a kinetic equation (117) which describes the evolution of fluctuations around a uniform static background. We now sketch the steps needed to extend our analysis to an expanding hydrodynamic background, referring to the literature for a more complete treatment [11]. First, we need to take into account that $N_0^{\alpha\alpha}(t)$ as well as $D_\alpha(t)$ will in general depend on t . Second, we have to introduce gradient terms which account for the expansion of the system. The explicit expression of such gradient terms is not important for the subsequent discussion. What is important, though, is that these terms are proportional to $1/\tau_Q$, where τ_Q is the expansion rate we introduced earlier. Therefore in an expanding fluid background, the hydro-kinetic equation takes the form (schematically)

$$\partial_t N^{\alpha\alpha}(t, \mathbf{k}) = -2D_\alpha(t) k^2 [N^{\alpha\alpha}(t, k) - N_0^{\alpha\alpha}(t)] + [\text{terms} \propto 1/\tau_Q]. \quad (122)$$

The dynamics of $N^{\alpha\alpha}$ as described by Eq. (122) is driven by the competition between the expansion of the system and the equilibration of thermal fluctuations. Since the equilibration of $N^{\alpha\alpha}$ is achieved by diffusion with rate $\propto Dk^2$, $N^{\alpha\alpha}$ will depend non-trivially on wavelength, although the equilibrium expectation $N_0^{\alpha\alpha}$ is k -independent. Away from the critical point, we can estimate a non-equilibrium length scale, $\ell_{\text{neq}} \sim \ell_{\text{max}}$, which divides the non-equilibrium and equilibrium fluctuations of the system, characterizing the transition between the two regimes. Wavelengths longer than ℓ_{max} are too long to equilibrate by diffusion over a time τ_Q . Recalling the introduction, we parametrize the diffusion constant away from the critical point as

$$D_0 \sim \frac{\ell_0^2}{\tau_0}, \quad (123)$$

where τ_0 is the microscopic relaxation time, and ℓ_0 is a microscopic length. Equating the diffusion rate of a mode of wavenumber $k \sim 1/\ell_{\max}$ with the expansion rate $\sim 1/\tau_Q$

$$D_0 k^2 \sim 1/\tau_Q, \quad (124)$$

we obtain Eq. (6) as advertised in the introduction.

As we discuss below, when the system approaches the critical point, the length scale ℓ_{neq} (which separates the non-equilibrium and equilibrium fluctuations of the system) will decrease, and a shorter length ℓ_{kz} will replace ℓ_{\max} .

2. Evolution of fluctuations in the hydrodynamic regime near a critical point

Let us now apply the general kinetic equation obtained in the previous section, Eq. (122), to a system passing close to the QCD critical point. Because of criticality two new features emerge which simplify Eq. (122). First, since $N_0^{\alpha\alpha}$ will become singular near a critical point, the percent change per time of $N_0^{\alpha\alpha}$ will become much larger than $1/\tau_Q$ (see below), and the gradient terms proportional to $1/\tau_Q$ in Eq. (122) can be safely neglected. Second, a hierarchy of relaxation rates emerges near a critical point with $D_{\hat{s}} \ll D_{\pm}$ [18]. This is because $D_{\hat{s}}$ is inversely proportional to C_p , which is the most divergent susceptibility near the critical point. Thus, the \hat{s} mode will be the first to fall out of equilibrium during a transit of the critical point. For these reasons, we will concentrate on the evolution of the $N^{\hat{s}\hat{s}}$ from now on, and write the equation for $N^{\hat{s}\hat{s}}$ from Eq. (122) as

$$\partial_t N^{\hat{s}\hat{s}}(t, \mathbf{k}) = -2D_{\hat{s}}(t)k^2 [N^{\hat{s}\hat{s}}(t, \mathbf{k}) - C_p(t)] . \quad (125)$$

Eq. (125) is valid in the hydrodynamic region $k \ll 1/\xi$. We will extend Eq. (125) to the scaling regime in the next section.

B. Evolution of fluctuations in the scaling regime near a critical point

Before continuing, let us review the equilibrium result for $N^{\hat{s}\hat{s}}$ which is notated with $N_0^{\hat{s}\hat{s}}$. As derived in Sect. II, the equilibrium correlator takes the form

$$N_0^{\hat{s}\hat{s}}(t, \mathbf{k}) = \frac{C_p(t)}{1 + (k\xi(t))^{2-\eta}} , \quad (126)$$

where $C_p(t) = \chi_{\text{is}}(t)/A_s^2$ and $\xi(t)$ are the time dependent susceptibility and correlation length respectively. The interpolating form for the k -dependence captures two limits: the low- k hydrodynamic limit $k\xi \ll 1$, and the high- k scaling limit $k\xi \gg 1$. In the high- k scaling limit, the equilibrium correlation functions are power laws $N_0^{\hat{s}\hat{s}} \propto k^{-(2-\eta)}$ and are independent of $\xi(t)$.

We will introduce a dynamical model to describe the non-equilibrium evolution of $N^{\hat{s}\hat{s}}(t, \mathbf{k})$ for the full range of momenta, including $k\xi \sim 1$. Using fluctuating hydrodynamics we derived a hydro-kinetic equation for $N^{\hat{s}\hat{s}}$ which applies in the hydrodynamic regime where $k \ll 1/\xi$. To generalize this relaxation equation to modes in the scaling regime $\xi^{-1} \ll k \ll \ell_0^{-1}$, let us first write the small k hydrodynamic equation (125) more explicitly

$$\partial_t N^{\hat{s}\hat{s}}(t, \mathbf{k}) = -2 \left(\frac{\lambda_T}{C_p} \right) k^2 [N^{\hat{s}\hat{s}}(t, \mathbf{k}) - C_p(t)] , \quad (k\xi \ll 1) . \quad (127)$$

Here λ_T is the thermal conductivity described in Sect. III A 1. Observe that the relaxation rate in Eq. (127) is proportional to the transport coefficient (i.e. λ_T) divided by the corresponding susceptibility (i.e. C_p). We expect this pattern will still hold for finite k . Thus, as a rough model for $k\xi \sim 1$ (called the “conventional theory” by Halperin and Hohenberg [34]), we will replace the specific heat in (127) with its k -dependent form

$$C_p \rightarrow \frac{C_p}{1 + (k\xi)^{2-\eta}}, \quad (128)$$

and treat the conductivity λ_T as a constant. In the context of QCD, a similar model was discussed and motivated by Son and Stepanov [35].

The model takes the form of a k -dependent relaxation time equation

$$\partial_t N^{\hat{s}\hat{s}}(t, \mathbf{k}) = -2\Gamma_{\hat{s}}(t, k) [N^{\hat{s}\hat{s}}(t, \mathbf{k}) - N_0^{\hat{s}\hat{s}}(t, k)], \quad (129)$$

where

$$\Gamma_{\hat{s}}(t, k) \equiv \left(\frac{\lambda_T}{C_p \xi^2} \right) (k\xi)^2 (1 + (k\xi)^{2-\eta}). \quad (130)$$

The model reduces to the hydrodynamic limit in (127) for $k\xi \ll 1$. It captures the general feature that high k modes equilibrate rapidly, and approach the equilibrium scaling form for $k\xi \gg 1$. Outside of these regimes it is just a model which misses some of the essential physics which we will discuss shortly.

When the system passes directly through the critical point, $t_{\text{cr}} \rightarrow 0$ with $t < 0$, the specific heat follows the power law (from eqs. (86) and (91))

$$C_p = \frac{\chi_0}{A_s^2} \left(\frac{\xi}{\ell_0} \right)^{2-\eta}, \quad (131)$$

and the relaxation rate for $k\xi = 1$ depends on the correlation length ξ as

$$\Gamma_{\hat{s}}(t, \xi^{-1}) = \frac{2}{\tau_0} \left(\frac{\xi}{\ell_0} \right)^{-4+\eta}, \quad (132)$$

where we have defined a typical microscopic timescale τ_0 using the previously defined constants

$$\frac{1}{\tau_0} \equiv A_s^2 \left(\frac{\lambda_T}{\chi_0 \ell_0^2} \right). \quad (133)$$

τ_0 and ℓ_0 set the diffusion coefficient away from the critical point, $D_0 \equiv \lambda_T/C_{p,0} = \ell_0^2/\tau_0$. For $k \gg \xi^{-1}$, the relaxation rate is large, scales with a power of k , and is independent of the correlation length

$$\Gamma_{\hat{s}}(t, k) \Big|_{k\xi \gg 1} = \frac{1}{\tau_0} (\ell_0 k)^{4-\eta}. \quad (134)$$

1. Discussion of the relaxation model of Eq. (129)

Eq. (129) is a heuristic relaxation model which captures the expected parametric dependencies on wavenumber and time. It is motivated by Model B in the Halperin and Hohenberg

classification scheme [34], which we briefly review to highlight the virtues and limitations of the relaxation model.

In Model B the order parameter evolves according to the nonlinear stochastic differential equation

$$\frac{d\psi(t, \mathbf{x})}{dt} = \lambda_0 \vec{\nabla} \cdot \left(\vec{\nabla} \frac{\delta F}{\delta \psi} \right) + \xi_\psi(t, \mathbf{x}), \quad (135)$$

where the noise satisfies

$$\langle \xi_\psi(t, \mathbf{k}) \xi_\psi(t', -\mathbf{k}') \rangle = 2\lambda_0 k^2 \delta^{(3)}(\mathbf{k} - \mathbf{k}') \delta(t - t'), \quad (136)$$

and the free energy functional is⁸

$$F[\psi, r(t), h(t)] = \int d^d \mathbf{x} \left(\frac{1}{2\tilde{\chi}_0} m^2(r(t)) \psi^2 + \frac{1}{2\tilde{\chi}_0} (\nabla \psi)^2 + c_4 \psi^4 \right) + h(t) \psi. \quad (137)$$

The parameter $m^2(r)$ depends linearly on the Ising reduced temperature r , e.g. in mean field theory $m^2(r) \propto r$. The dependence on r in $m^2(r)$ is determined by the equilibrium equation of state and is not modified by the expansion of the system⁹. Even when the system is expanding and out of equilibrium, the Ising reduced temperature and field, $r(t)$ and $h(t)$, are related to the QCD parameters $e(t)$ and $n(t)$ with the equilibrium equation of state and the linear map described in Sect. II A. This is the Landau frame choice in hydrodynamics [20]. For an adiabatic expansion $e(t)$ and $n(t)$ depend linearly on time as specified in Sect. I B.

Since $\delta \hat{s}(t, \mathbf{x})$ has overlap with the order parameter ψ , the fluctuations in \hat{s} are dominated by fluctuations in the order parameter. Indeed, in the simple mapping of Sect. II A we find

$$\delta \hat{s}(t, \mathbf{x}) \simeq \frac{\delta \psi(t, \mathbf{x})}{A_s}, \quad (138)$$

up to corrections which are less singular near the critical point. Away from the critical point $m^2(r)$ is large, and the kinetic and quartic terms can be neglected. The equation of motion for ψ or \hat{s} then reduces to the hydrodynamic result, $\partial_t \hat{s} \propto \nabla^2 \hat{s}$, with the kinetic term $(\nabla \psi)^2$ in the free energy giving rise to a negligible higher-derivative correction to the diffusion equation.

In mean field theory the quartic coupling is neglected¹⁰, and the mass parameter (or inverse correlation length) goes to zero, $m^2(r) \equiv \xi^{-2}(r) \propto r$. The Ising specific heat scales as $\chi_{\text{is}} \propto \tilde{\chi}_0 \xi^2$, and the equilibrium correlation function is

$$\langle \psi(\mathbf{k}) \psi(-\mathbf{k}') \rangle = (2\pi)^3 \delta^{(3)}(\mathbf{k} - \mathbf{k}') \frac{\tilde{\chi}_0}{m^2(r) + k^2}. \quad (139)$$

If only quadratic fluctuations are included, the equation of motion for ψ reads

$$\frac{d\psi(t, \mathbf{k})}{dt} = -\frac{\lambda_0}{\tilde{\chi}_0} k^2 (m^2(r) + k^2) \psi(t, \mathbf{k}) + \xi_\psi. \quad (140)$$

⁸ We put here $\tilde{\chi}_0$ instead of χ_0 because $\tilde{\chi}_0$ differs from the χ_0 used in the rest of the paper by an unimportant constant.

⁹ This is because the parameters m , $\tilde{\chi}$, and c_4 are determined by integrating out high momentum modes which are always close to equilibrium. For a discussion of this point and Landau matching in the context of stochastic hydrodynamics see Ref. [20].

¹⁰ For simplicity we will describe the symmetric phase with $h = 0$ where $\langle \psi \rangle = 0$.

This evolution has the same form as Eq. (129), and provides the motivation for using Eq. (129) as a model. At large k the damping rate is independent of the correlation length, and scales as $\Gamma(k) \sim k^z$ with a dynamical critical exponent of $z = 4$.

Of course the quartic coupling can not be ignored near the critical point. Including the quartic coupling changes the equilibrium mean field exponents to their observed values. Further, an analysis of asymptotics of the equilibrium response functions in Model B at large k shows that quartic couplings change the dynamical critical exponent from the mean field result to $z = 4 - \eta$ [34]. However, at small k the non-linear interactions do not renormalize the conductivity [34], and thus fluctuations in equilibrium at small k evolve according to the stochastic diffusion equation

$$\frac{d\psi(t, \mathbf{k})}{dt} = -\frac{\lambda_0}{\chi_{\text{is}}} k^2 \psi_{\mathbf{k}} + \xi_{\psi}, \quad (141)$$

where $\chi_{\text{is}} \propto \tilde{\chi}_0 \xi^{2-\eta}$. Thus as in the model of Eq. (129), the conductivity λ_0 of Model B remains finite as we approach the critical point. The model in Eq. (129) also has the correct equilibrium static and dynamical critical exponents put in by hand in order to account for some of the interactions between the modes. In the expanding situation, this is clearly just a model – the four and higher point functions will not be in equilibrium, and must also be evolved to determine their influence on the two point functions. Nevertheless, in the epsilon expansion the quartic coupling is perturbatively small, and including higher point functions should only perturbatively modify the model's parametric predictions.

We have described Model B where the momentum fluctuations are neglected. In Model H the coupling between the momentum \vec{g} and the order parameter ψ is included [34], and this model will fully describe the QCD critical point¹¹. In this case the conductivity λ_T will scale with the correlation length ξ as

$$\lambda_T = \lambda_0 \left(\frac{\xi}{\ell_0} \right)^{x_\lambda}, \quad x_\lambda \simeq 0.95, \quad (142)$$

where λ_0 is the typical thermal conductivity away from the critical point, and the exponent x_λ results from the renormalization of the conductivity by the momentum fluctuations of the system [35]. Such a renormalization (which ultimately is a resummation of the non-linear interactions of the stochastic system) is neglected in the current model. In addition, the renormalized conductivity will in general depend on k as $\lambda_T K_\lambda(k\xi)$, where $K_\lambda(k\xi)$ is another dynamical scaling function with fixed normalization, $K_\lambda(0) = 1$. The scaling function $K_\lambda(k\xi)$ has been studied extensively [26, 36, 37], and its asymptotic behavior is also related to critical exponent x_λ

$$K_\lambda(k\xi) \sim (k\xi)^{-x_\lambda}, \quad k\xi \gg 1. \quad (143)$$

Thus, the relaxation rate at large k is generally expected to scale with the dynamical critical exponent $z \equiv 4 - \eta - x_\lambda$

$$\Gamma_s(t, k) \Big|_{k\xi \gg 1} \sim \frac{1}{\tau_0} (\ell_0 k)^z, \quad z \equiv 4 - \eta - x_\lambda. \quad (144)$$

¹¹ Model H is essentially contained in stochastic hydrodynamics, provided a kinetic term $(\nabla\psi)^2$ is added to the free energy functional [24, 26, 34], which in turn modifies the equation of motion by a particular higher derivative correction.

In comparison with Eq. (144), the current model (134) has the dynamical critical exponent

$$z = 4 - \eta, \quad (145)$$

which we will use in the numerical work below. While it is straightforward to refine the model and to input x_λ and K_λ from Model H, we will continue to use the Model B results, which are sufficient for our illustrative purpose. It would be interesting to simulate a stochastic non-linear Landau-Ginzburg functional which would naturally reproduce the correct dynamical critical exponents of Model H, and correctly describe the non-linear and non-equilibrium evolution of the system during the expansion.

C. Kibble-Zurek scaling and missing the critical point

Before solving Eq. (130) numerically, let us analyze the timescales associated with this evolution. As noted in the previous subsection, low momentum modes with $k \ll \xi^{-1}$ have a small relaxation rate and are out-of-equilibrium even away from the critical point. On the other hand, high momentum modes with $k \gg \xi^{-1}$ have a large relaxation rate and are always in equilibrium. We will focus on modes with $k \sim \xi^{-1}$ where the relaxation rate as a function of time follows the pattern described in Sect. II C for $\chi(t)$ and $\xi(t)$ (see Eq. (130)). Specifically, from eqs. (86), (91), and (130), $\Gamma_{\hat{s}}$ takes the form

$$\Gamma_{\hat{s}}(t, \xi^{-1}) = \frac{1}{\tau_0} \left(\frac{|t|}{\bar{\tau}_Q} \right)^{avz} f_\Gamma \left(\frac{t}{|t_{\text{cr}}|} \right), \quad (146)$$

where

$$f_\Gamma \equiv \frac{1}{f_\chi f_\xi^2}. \quad (147)$$

is a universal function. Following the pattern described in Sect. II C, f_Γ has the following limits

$$f_\Gamma(u) = \begin{cases} 1 & u < -1, \\ f_\Gamma^+ \equiv 0.3427 & u \rightarrow +\infty, \end{cases} \quad (148)$$

and $|u|^{avz} f_\Gamma(u)$ is regular for $u > -1$.

Examining the relaxation time equation (129), the dynamical evolution of $N^{\hat{s}\hat{s}}(t, k)$ is controlled by a competition between the relaxation rate $\Gamma_{\hat{s}}(t, k)$ and the rate of change of the equilibrium expectation $N_0^{\hat{s}\hat{s}}(t, k)$. First we analyze the limit $t_{\text{cr}} \rightarrow 0$ and $t < 0$, where the relaxation rate takes the scaling form

$$\Gamma_{\hat{s}}(t, \xi^{-1}) = \frac{1}{\tau_0} \left(\frac{|t|}{\bar{\tau}_Q} \right)^{avz}, \quad (149)$$

reflecting the equilibrium scaling of χ and ξ in this limit

$$C_p = \frac{\chi_0}{A_s^2} \left(\frac{|t|}{\bar{\tau}_Q} \right)^{-a\gamma}, \quad (150)$$

$$\xi = \ell_0 \left(\frac{|t|}{\bar{\tau}_Q} \right)^{-a\nu}. \quad (151)$$

For $t > 0$ these forms are multiplied by the order one factors, f_Γ^+ , f_χ^+ and f_ξ^+ , respectively. When $t \rightarrow 0$, the system approaches the critical point, and the relaxation rate decreases exhibiting critical slowing down. By contrast, the percent change per time of the equilibrium susceptibility C_p is of order

$$\left| \frac{\partial_t C_p}{C_p} \right| \sim \left| \frac{1}{t} \right|, \quad (152)$$

which diverges near the critical point. Consequently, the system will inescapably fall off equilibrium at some time t_{kz} (the Kibble-Zurek time), which can be determined by comparing these competing rates

$$\frac{1}{t_{\text{kz}}} = \frac{1}{\tau_0} \left(\frac{t_{\text{kz}}}{\bar{\tau}_Q} \right)^{a\nu z}. \quad (153)$$

Solving for t_{kz} we find

$$t_{\text{kz}} = \tau_0 \left(\frac{\tau_0}{\bar{\tau}_Q} \right)^{-a\nu z/(a\nu z+1)}, \quad (154)$$

which is an intermediate scale $\tau_0 \ll t_{\text{kz}} \ll \bar{\tau}_Q$. Indeed, since $\bar{\lambda} \equiv \tau_0/\bar{\tau}_Q \ll 1$, the timescales τ_0 , t_{kz} , and $\bar{\tau}_Q$ are widely separated:

$$\bar{\lambda} \ll \bar{\lambda}^{1/(a\nu z+1)} \ll 1. \quad (155)$$

The Kibble-Zurek time t_{kz} characterizes the temporal evolution of $N^{\hat{s}\hat{s}}$ during a transit of the critical point. Let us introduce an associated length scale ℓ_{kz} (the Kibble-Zurek length), which is defined as the value of correlation length ξ at $t = -t_{\text{kz}}$

$$\ell_{\text{kz}} \equiv \ell_0 \left(\frac{\tau_0}{\bar{\tau}_Q} \right)^{-a\nu/(a\nu z+1)} = \ell_0 \bar{\lambda}^{-a\nu/(a\nu z+1)}. \quad (156)$$

Modes with $k \lesssim \ell_{\text{kz}}^{-1}$ will fall out equilibrium for $|t| \sim t_{\text{kz}}$, while modes with $k \gg \ell_{\text{kz}}^{-1}$ will remain equilibrated. We therefore expect that ℓ_{kz} will characterize the momentum dependence of $N^{\hat{s}\hat{s}}(t, k)$. ℓ_{kz} is also an intermediate scale, $\ell_0 \ll \ell_{\text{kz}} \ll \ell_{\text{max}} \sim \ell_0 \lambda^{-1/2}$, where ℓ_{max} is the maximum wavelength that can be equilibrated away from the critical point.

Finally, since the evolution is “frozen” for $t \gtrsim -t_{\text{kz}}$, the magnitude of $N^{\hat{s}\hat{s}}(t, k)$ can be estimated by the value of C_p at $t = -t_{\text{kz}}$

$$N^{\hat{s}\hat{s}} \sim \frac{\chi_{\text{kz}}}{A_s^2} \equiv C_{p,\text{kz}}, \quad \chi_{\text{kz}} \equiv \chi_0 \left(\frac{\ell_{\text{kz}}}{\ell_0} \right)^{2-\eta}. \quad (157)$$

Thus, ℓ_{kz} also determines the magnitude of fluctuations during a transit of the critical point through the definition of $\chi_{\text{kz}} \propto \ell_{\text{kz}}^{2-\eta}$.

The qualitative discussion in the preceding paragraphs motivates us to introduce a rescaled two point function

$$N^{\hat{s}\hat{s}} \equiv \frac{\chi_{\text{kz}}}{A_s^2} \bar{N}^{\hat{s}\hat{s}}(\bar{t}, k\ell_{\text{kz}}; t/|t_{\text{cr}}|), \quad (158)$$

where we anticipate $\bar{N}^{\hat{s}\hat{s}}$ will be of order unity, and will depend on the rescaled time

$$\bar{t} \equiv \frac{t}{t_{\text{kz}}}. \quad (159)$$

Substituting (158) into (129), we obtain an equation for $\bar{N}^{\hat{s}\hat{s}}$:

$$\partial_{\bar{t}} \bar{N}^{\hat{s}\hat{s}} = -2 |\bar{t}|^{a\nu z} \frac{(k\xi)^2}{K_\chi(k\xi)} [\bar{N}^{\hat{s}\hat{s}} - |\bar{t}|^{-a\gamma} K_\chi(k\xi)] \quad \bar{t} \leq -t_{\text{cr}}/t_{\text{kz}}, \quad (160a)$$

$$\partial_{\bar{t}} \bar{N}^{\hat{s}\hat{s}} = -2 |\bar{t}|^{a\nu z} f_\Gamma \frac{(k\xi)^2}{K_\chi(k\xi)} [\bar{N}^{\hat{s}\hat{s}} - |\bar{t}|^{-a\gamma} f_\chi K_\chi(k\xi)] \quad \bar{t} \geq -t_{\text{cr}}/t_{\text{kz}}, \quad (160b)$$

where

$$k\xi = \begin{cases} k\ell_{\text{kz}} |\bar{t}|^{-a\nu} & \bar{t} \leq -t_{\text{cr}}/t_{\text{kz}} \\ k\ell_{\text{kz}} |\bar{t}|^{-a\nu} f_\xi & \bar{t} \geq -t_{\text{cr}}/t_{\text{kz}} \end{cases}, \quad (160c)$$

and K_χ is given Eq. (54). The three scaling functions f_Γ , f_χ and f_ξ take the form

$$f_\Gamma \left(\frac{t_{\text{kz}}}{|t_{\text{cr}}|} \bar{t} \right), \quad f_\chi \left(\frac{t_{\text{kz}}}{|t_{\text{cr}}|} \bar{t} \right), \quad f_\xi \left(\frac{t_{\text{kz}}}{|t_{\text{cr}}|} \bar{t} \right). \quad (160d)$$

Thus, $\bar{N}^{\hat{s}\hat{s}}$ only depends on scaling variables $\bar{t} = t/t_{\text{kz}}$, $k\ell_{\text{kz}}$ and $t_{\text{kz}}/t_{\text{cr}}$. When the system passes directly through the critical point $t_{\text{cr}} \rightarrow 0$, the quantities f_Γ , f_χ and f_ξ approach universal constants (f_Γ^+ , f_χ^+ , and f_ξ^+), and the correlation function $N^{\hat{s}\hat{s}}$ is only a function of t/t_{kz} and $k\ell_{\text{kz}}$. When the system misses the critical point by an amount Δ_s there is an additional time scale $t_{\text{cr}} \propto \tau_Q \Delta_s^b$, and the correlation function for $t > -t_{\text{cr}}$ additionally depends on the ratio $t_{\text{cr}}/t_{\text{kz}}$. We will present numerical results for $\bar{N}^{\hat{s}\hat{s}}$ in the next section by solving Eq. (160).

D. Transits of a critical point: numerical evaluation

Now we will determine $N^{\hat{s}\hat{s}}$ by solving Eq. (160) numerically¹². First, we evaluate $N^{\hat{s}\hat{s}}$ when the system passes directly through the critical point by setting t_{cross} to zero. In Fig. 3(a) and (b) we plot $\bar{N}^{\hat{s}\hat{s}}$ as function of k for representative times before and after the critical point respectively. For comparison, we plot the corresponding equilibrium expectation with dashed curves.

As seen in the figure, the fluctuations recorded by $N^{\hat{s}\hat{s}}$ are maximal at a given wavenumber k_{neq} corresponding to a definite wavelength, $\ell_{\text{neq}} \equiv k_{\text{neq}}^{-1} \sim \ell_{\text{kz}}$. This is in contrast with the behavior of the equilibrium fluctuations $N_0^{\hat{s}\hat{s}}$ (the dashed curves) which increase monotonically as $k \rightarrow 0$. The maximum is the result of a competition between the hydrodynamic behavior at small k , and the critical scaling behavior at large k . Modes with $k \ll \ell_{\text{neq}}^{-1}$ equilibrate slowly (diffusively), reflecting the fact that the total charge is conserved and does not fluctuate. Consequently, the system does not respond to the increasing critical susceptibility at small k , and the magnitude of $N^{\hat{s}\hat{s}}$ in the hydrodynamic region remains small compared to the equilibrium specific heat C_p . At large k , the relaxation rate grows as k^z and becomes very large. Thus, the large k tail of $N^{\hat{s}\hat{s}}$ is always close to the equilibrium expectation, which vanishes as $1/k^{2-\eta}$. To summarize, $N^{\hat{s}\hat{s}}$ will become small at both small

¹² We need to specify the initial conditions of $N^{\hat{s}\hat{s}}$ at an initial time t_I/t_{kz} , where $t_I < 0$ is the time when system enters the critical region. However, we are working in the parametric regime where $\tau_Q/t_{\text{kz}} \rightarrow \infty$, and the time t_I is of order τ_Q . Therefore, t_I/t_{kz} should be taken to negative infinity; we take $t_I/t_{\text{kz}} \sim -40$ in practice. Non-equilibrium effects will not be important at this early time, and consequently we initialize $N^{\hat{s}\hat{s}}$ in equilibrium.

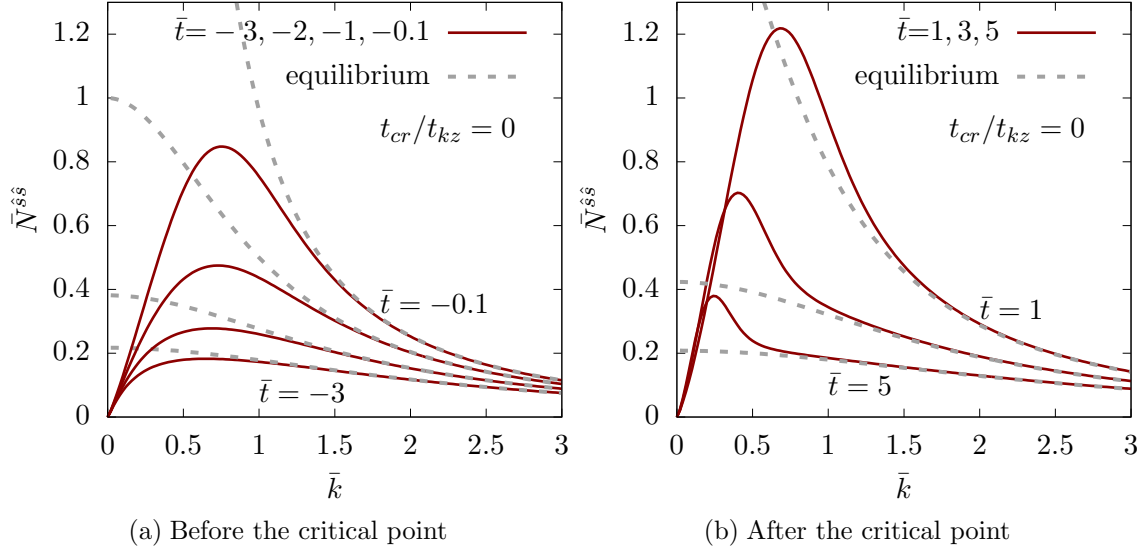


FIG. 3. The time evolution of the correlation function of entropy per baryon fluctuations $\delta\hat{s} \equiv \delta s - (s/n)\delta n$, when the system passes directly through the critical point, $t_{\text{cr}}/t_{\text{kz}} = 0$. The wavenumber is measured in units of ℓ_{kz}^{-1} ($\bar{k} \equiv k\ell_{\text{kz}}$), and $N^{\hat{s}\hat{s}}$ has been rescaled by the specific heat C_p at the Kibble-Zurek time $C_{p,\text{kz}}$ ($\bar{N}^{\hat{s}\hat{s}} \equiv N^{\hat{s}\hat{s}}/C_{p,\text{kz}}$). (a) The time evolution in the coexistence region $t < 0$ (before the critical point). (b) The time evolution after the system has left the coexistence region $t > 0$ (after the critical point).

k and large k , naturally exhibiting maximum at some intermediate wavenumber ℓ_{neq}^{-1} . This scale characterizes $N^{\hat{s}\hat{s}}$ in the sense that wavenumbers significantly larger than ℓ_{neq}^{-1} are in equilibrium, while those smaller than ℓ_{neq}^{-1} are out of equilibrium.

From Fig. 3, the fluctuations grow with time for $t < 0$, and then return to their typical size after passing the critical point, $t > 0$. However, as we approach the critical point, the growth in $N^{\hat{s}\hat{s}}$ for $t > -t_{\text{kz}}$ is modest when compared to the rapid growth of C_p (the dashed curves at $k = 0$). The system is exhibiting critical slowing down, and lags behind its equilibrium expectation.

The slow evolution of $N^{\hat{s}\hat{s}}$ implies that the system can remember the magnitude of the critical fluctuations even after passing through the critical point. Indeed for $\bar{t} > 0$, $N_{\text{max}}^{\hat{s}\hat{s}}$ is even larger than its equilibrium expectation. Similar observations about the “memory effect” of critical fluctuations have been made in previous studies [9, 10]. The distinctive feature of $N^{\hat{s}\hat{s}}$, namely the maximum at a specific wavenumber ℓ_{neq}^{-1} , is remembered for $\bar{t} > 0$. It remains to be seen which experimental observables provide access to this interesting structure – see Sec. IV 4 for a preliminary proposal.

We now turn to finite detuning case shown in Fig. 4. In Fig. 4 (a,b), we show our results for $N^{\hat{s}\hat{s}}$ at $t_{\text{cr}}/t_{\text{kz}}=1$. The qualitative features are similar to the $t_{\text{cr}}/t_{\text{kz}}=0$ case, but the magnitude of the fluctuations is reduced. For still larger detuning $t_{\text{cr}}/t_{\text{kz}}=3$ shown in (c,d), the fluctuations are reduced even further. In the large detuning regime the equilibrium scaling of the specific heat at the crossing time t_{cr} determines the magnitude of the fluctuations rather than the relaxation dynamics. Thus, the magnitude of the critical fluctuations are independent of λ in this regime. Straightforward analysis based the previous sections (see

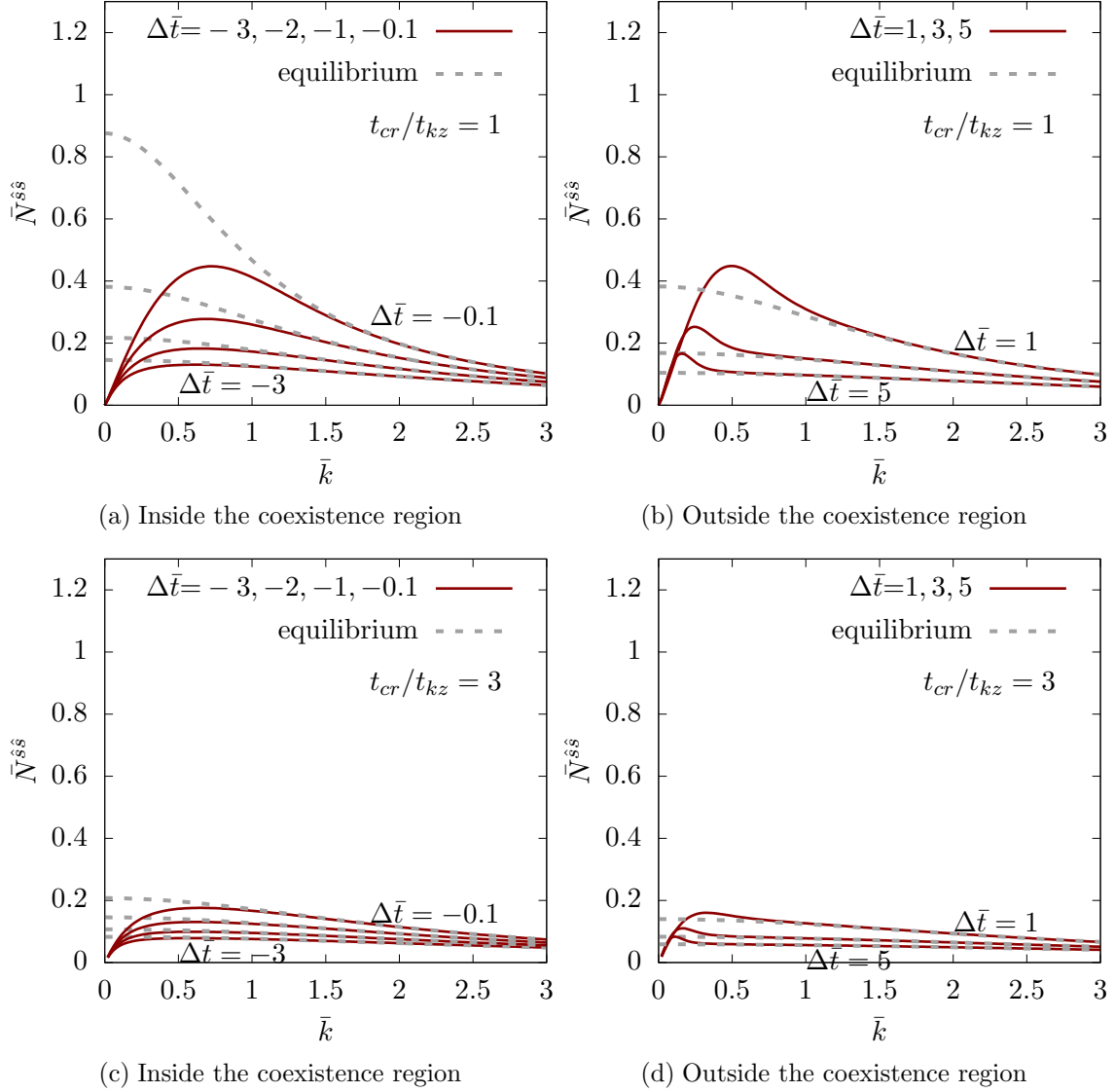


FIG. 4. (The upper row): The same as Fig. 3, but the system misses the critical point with $t_{cr}/t_{kz} = 1$. t_{cr} is the time when the system leaves the coexistence region, and $\Delta t \equiv t - t_{cr}$. (a) The time evolution of $N^{\hat{s}\hat{s}}$ when the system is in the coexistence region $t < t_{cr}$, and (b) when the system leaves the coexistence region $t > t_{cr}$. (The lower row): The same as the upper row, but with $t_{cr}/t_{kz} = 3$.

Sect. IIC) shows that at t_{cr} the fluctuations are of order

$$N^{\hat{s}\hat{s}} \sim C_{p,kz} \left(\frac{t_{cr}}{t_{kz}} \right)^{-a\gamma} \sim \frac{\chi_0}{A_s^2} \bar{\Delta}_s^{-\gamma/\beta}. \quad (161)$$

The wavenumber ℓ_{neq}^{-1} where the system transitions from the non-equilibrium behavior at small k to equilibrium behavior at large k is also reduced relative to ℓ_{kz}^{-1} . Equating the relaxation rate at the crossing time to the rate of change in equilibrium, $\Gamma(t_{cr}, k_{neq}) \sim t_{cr}^{-1}$,

shows that

$$\ell_{\text{neq}} \sim \ell_{\text{kz}} \left(\frac{t_{\text{cr}}}{t_{\text{kz}}} \right)^{(a\nu(z-2)+1)/2} \sim \ell_0 \lambda^{-1/2} \bar{\Delta}_s^{(a\nu(z-2)+1)/2a\beta}. \quad (162)$$

Numerically these exponents evaluate to

$$N^{\hat{s}\hat{s}} \sim \frac{\chi_0}{A_s^2} \bar{\Delta}_s^{-3.8}, \quad (163)$$

$$\ell_{\text{neq}} \sim \ell_0 \lambda^{-1/2} \bar{\Delta}_s^{3.26}. \quad (164)$$

When the detuning Δ_s approaches unity, the non-equilibrium length ℓ_{neq} approaches $\ell_{\text{max}} = \ell_0 \lambda^{-1/2}$. Modes with wavelength longer than ℓ_{max} remember the initial conditions at $t = -\tau_Q$, and are unaffected by the transit of the critical point.

Summarizing this subsection, we have evaluated the fluctuations in the entropy to baryon number, $N^{\hat{s}\hat{s}}$, for a system which passes directly through the critical point ($t_{\text{cr}}/t_{\text{kz}}=0$), and which misses the critical point ($t_{\text{cr}}/t_{\text{kz}} \neq 0$). When $t_{\text{cr}}/t_{\text{kz}}$ is not significantly larger than unity, the wavenumber dependence of $N^{\hat{s}\hat{s}}$ is qualitatively different from its equilibrium expectation, and from earlier work. Previously, the non-equilibrium variance of the order parameter field has been evaluated for “model A” [15]. In this case the order parameter is not conserved, and its relaxation rate remains finite at $k = 0$. By contrast, the order parameter for QCD is conserved, and the relaxation rate vanishes as $k \rightarrow 0$. Because of this fundamental difference $N^{\hat{s}\hat{s}}$ develops a maximum around $k \sim \ell_{\text{kz}}^{-1}$, and the critical fluctuations will be most pronounced at the corresponding wavelength $\sim \ell_{\text{kz}}$. This feature is absent in the study of Ref. [15].

IV. DISCUSSION

In this paper we have studied how the QCD medium created in a heavy ion collision will evolve during a transit of the conjectured critical point. We have defined two parameters, which are repeated here for convenience. The first is the “detuning parameter”

$$\Delta_s \equiv \frac{n_c}{s_c} \left(\frac{s}{n} - \frac{s_c}{n_c} \right), \quad (165)$$

and the second is the ratio of the microscopic time scale τ_0 to the expansion rate τ_Q^{-1}

$$\lambda \equiv \tau_0 \partial_\mu u^\mu \equiv \frac{\tau_0}{\tau_Q}. \quad (166)$$

Then we asked how the critical hydrodynamic fluctuations in the system depend on these two parameters during the transit. These two parameters quantify how missing the critical point and finite relaxation rates will regulate the growth of critical fluctuations. This conclusion is organized around explaining Fig. 5 which summarizes our results.

1. Object of study and its behavior away from the critical point

First we explained that observable of primary interest is the fluctuations in the entropy per baryon (multiplied by n)

$$\hat{s} \equiv n \delta \left(\frac{s}{n} \right) = \delta s - \frac{s}{n} \delta n. \quad (167)$$

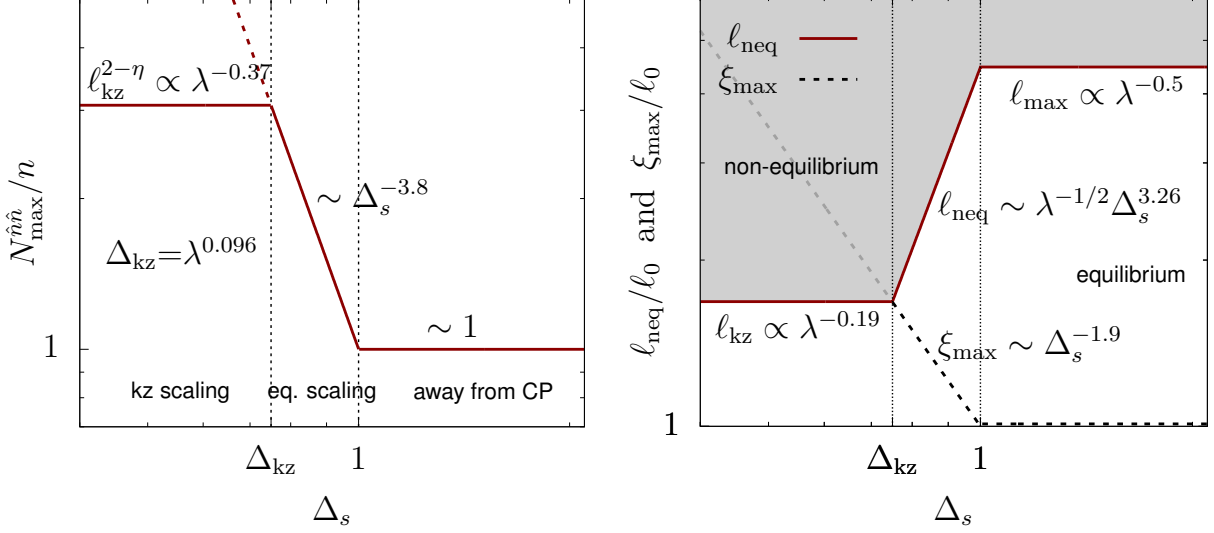


FIG. 5. A schematic plot showing the dependence of the maximal fluctuations, $N_{\max}^{\hat{n}}/n$, and the maximal correlation length, ξ_{\max} , on the parameters Δ_s and λ during a transit of the critical point. Also shown is the non-equilibrium length ℓ_{neq} – modes with wavelength longer than ℓ_{neq} fall out of equilibrium during the transit. For $\Delta_s \gtrsim 1$ the adiabatic trajectory misses the critical point completely. In this regime $N_{\max}^{\hat{n}}/n$ is of order unity, and ℓ_{neq} is of order $\ell_{\max} \sim \ell_0 \lambda^{-1/2}$. For $\Delta_s < 1$, but larger than $\Delta_{kz} = \lambda^{0.096}$, the trajectory approaches the critical point. In this (narrow) regime the dependence of $N_{\max}^{\hat{n}}/n$ and ξ_{\max} on Δ_s follows from equilibrium scaling. The non-equilibrium length ℓ_{neq} remains longer than the correlation length ξ_{\max} . For $\Delta_s \lesssim \Delta_{kz}$, equilibrium scaling is irrelevant, and the Kibble-Zurek scaling sets in. In Kibble-Zurek region $N_{\max}^{\hat{n}}/n$ and ℓ_{neq} scale as $\lambda^{-0.37}$ and $\ell_0 \lambda^{-0.19}$ respectively. In this region, both quantities are independent Δ_s , i.e. of how close the adiabatic trajectory is to the critical point.

From an experimental point of view, it may be easier to work with the fluctuations in the baryon number per entropy (multiplied by s) :

$$\delta \hat{n} \equiv s \delta \left(\frac{n}{s} \right) = \delta n - \frac{n}{s} \delta s. \quad (168)$$

which contains the same physical content.

We determined the time evolution near the critical point of the equal time correlation functions of $\delta \hat{n}$

$$N^{\hat{n}\hat{n}}(t, \mathbf{k}) \equiv \int d^3x e^{i\mathbf{k}\cdot\mathbf{x}} \langle \delta \hat{n}(t, \mathbf{x}) \delta \hat{n}(t, \mathbf{0}) \rangle. \quad (169)$$

In the body of the text we have worked with $N^{\hat{s}\hat{s}}(t, \mathbf{k})$ which is proportional $N^{\hat{n}\hat{n}}(t, \mathbf{k})$

$$N^{\hat{n}\hat{n}}(t, \mathbf{k}) = \left(\frac{n}{s} \right)^2 N^{\hat{s}\hat{s}}(t, \mathbf{k}). \quad (170)$$

$N^{\hat{n}\hat{n}}$ encodes the spatial correlations amongst the baryons that existed just before the freeze-out process. Unfortunately, currently we do not have a precise prescription for how to use this equal time correlator in conjunction with Cooper-Frye freezeout or other procedure to determine the momentum space correlations amongst the produced baryons after the freezeout process.

Nevertheless, there are several reasons (discussed in Sect. II B 3 and Sect. III A 1) why $N^{\hat{n}\hat{n}}$ is the relevant quantity both theoretically and experimentally. First, $\delta\hat{n}$ is an eigenmode of linearized hydrodynamics, and its fluctuations are proportional to the specific heat at constant pressure. Specifically in equilibrium $N^{\hat{n}\hat{n}}$ determines C_p from its small k limit

$$N_0^{\hat{n}\hat{n}}(t, \mathbf{0})|_{\text{eq}} = V \langle (\delta\hat{n})^2 \rangle|_{\text{eq}} = \left(\frac{n}{s}\right)^2 C_p. \quad (171)$$

As the temperature approaches its critical value, $(n/s)^2 C_p$ will always diverge with the largest critical exponent of the Ising susceptibility matrix, $\gamma \simeq 1.23$. By contrast, the squared speed of sound approaches zero with the critical exponent $\alpha \simeq 0.11$, which is too slow to be of practical interest for the heavy ion program. As discussed in Sect. II B, these statements about C_p and c_s^2 are independent of the detailed mapping matrix between the QCD and Ising variables.

Now let us describe the behavior of $N^{\hat{n}\hat{n}}$ away from the critical point as illustrated in Fig. 5. Away from the critical point, the fluctuations in $\delta\hat{n}$ scale as the fluctuations in δn , which can be reasonably expected to be roughly Poissonian, $V \langle (\delta n)^2 \rangle \sim n$. This leads to a Poisson estimate for these fluctuations¹³

$$\frac{N^{\hat{n}\hat{n}}(t, \mathbf{k})}{n} \sim 1, \quad \text{with} \quad \ell_{\text{max}}^{-1} \ll k \ll \ell_0^{-1}. \quad (172)$$

Here ℓ_0 denotes a typical microscopic length scale, and ℓ_{max} is discussed below. Searches for critical fluctuations will look for enhancements at fixed k to this baseline expectation that change non-monotonically with the (mean) n/s .

Note that the Poissonian expectation in Eq. (172) is independent of k for all equilibrated modes with wavenumber smaller than the inverse correlation length $\sim \ell_0^{-1}$. As discussed in the introduction, modes with wavelength longer than a “non-equilibrium” length, $\ell_{\text{neq}} \sim \ell_{\text{max}} \sim \ell_0 \lambda^{-1/2}$, are always out of equilibrium even away from the critical point [11], and will not show critical behavior. We will see that when the system approaches the critical point, modes with wavelength shorter than ℓ_{max} will begin to fall out of equilibrium, and the non-equilibrium length ℓ_{neq} will decrease. This shown by the grey region of Fig. 5(b).

2. How missing the critical point regulates the critical fluctuations

In Sect. II C we determined how the equilibrium susceptibilities in QCD are regulated in time as the medium passes close the critical point during an adiabatic expansion with a detuning parameter Δ_s . This time evolution follows a specific pattern, which is a reflection of the scaling of the equilibrium equation of state. For example, the equilibrium specific heat $(n/s)^2 C_p$ (which diverges like the Ising susceptibility $\chi_{\text{is}} \propto r^{-\gamma}$) has the following time dependence for an adiabatic trajectory near the critical point

$$N_0^{\hat{n}\hat{n}}(t, \mathbf{0})|_{\text{eq}} = c_0 n \left| \frac{t}{\tau_Q} \right|^{-a\gamma} f_\chi \left(\frac{t}{|t_{\text{cr}}|} \right). \quad (173)$$

¹³ For example, we may estimate $N^{\hat{n}\hat{n}}$ for a hadron gas. For a hadron gas at a temperature of $T \simeq 155$ and $s/n \simeq 25$ (corresponding to the chemical freezeout conditions at $\sqrt{s_{NN}} = 12.5$ GeV) we find $nC_p/s^2 = 0.65$.

Here $f_\chi(t/|t_{\text{cr}}|)$ is a known universal scaling function of order unity which can be determined by the (R, θ) parameterization of the Ising Model susceptibility. c_0 is a dimensionless and order one non-universal constant, and the “crossing time” is

$$t_{\text{cr}} \equiv -c_1 \tau_Q \Delta_s^{1/a\beta} < 0, \quad (174)$$

where c_1 is another (dimensionless and order one) non-universal constant¹⁴. $t/|t_{\text{cr}}|$ plays the role of the scaling variable, and the scaling function $f_\chi(t/|t_{\text{cr}}|)$ approaches a (universal) constant for $t/|t_{\text{cr}}| \rightarrow \pm\infty$. From Eq. (173) we see that the specific heat grows like a power until the scaling variable $t/|t_{\text{cr}}|$ approaches -1 . For $t/|t_{\text{cr}}| \sim -1$ the system becomes aware that adiabatic trajectory will miss the critical point by Δ_s , and this stops the growth of the specific heat. Setting t to t_{cr} , we can estimate the maximum magnitude of equilibrium critical fluctuations relative to the Poissonian expectation

$$\frac{N_0^{\hat{n}}(t, \mathbf{k})}{n} \sim \Delta_s^{-\gamma/\beta}, \quad (175)$$

Here the wavelengths of interest k^{-1} are of order the correlation length at the crossing time

$$k^{-1} \sim \xi(t_{\text{cr}}) \sim \ell_0 \Delta_s^{-\nu/\beta}. \quad (176)$$

Sufficiently long wavelength modes are always out of equilibrium and will not show the enhancement in Eq. (175). Sect. IIID estimates that for Δ_s small (but larger than a Δ_{kz} discussed below) the non-equilibrium length is of order $\ell_{\text{neq}} \sim \ell_0 \lambda^{-1/2} \Delta_s^{3.26}$. Fig. 5 shows how the correlation length $\xi(t_{\text{cr}})$ and the non-equilibrium length ℓ_{neq} come together as we begin to approach the critical point.

The estimate in Eq. (175) realizes one of the goals of this paper, i.e. to parametrically estimate how missing the critical point limits the critical fluctuations. However, the analysis in the next section shows (unfortunately) that non-equilibrium physics will set in well before the critical fluctuations are regulated by a finite missing parameter Δ_s . Thus, the non-equilibrium dynamics will regulate the critical fluctuations well below the equilibrium estimate in Eq. (175). For this reason we will refrain from substituting numbers into Eq. (175).

3. How critical slowing down regulates the critical fluctuations

In Sect. III we estimated how the finite relaxation time limits the growth of critical fluctuations. For conserved (or approximately conserved) quantities such as n/s the relaxation time depends on the wavelength of the mode of interest, with longer wavelengths modes taking longer to relax. For $k \sim \xi^{-1}$, the typical relaxation time increases near the critical point as

$$\tau_R(\xi) \equiv \tau_0 \left(\frac{\xi}{\ell_0} \right)^z, \quad (177)$$

¹⁴ Explicit expressions for these constants are given in the text ($c_0 = 0.365 A_n^{-a\gamma}$ and $c_1 = A_s^b/A_n$) in terms of the mapping matrix M_b^A between the QCD and Ising variables described in Sect. IIA.

where $z \equiv 4 - \eta \simeq 4$ in our setup¹⁵, and τ_0 is the microscopic time. We then find that modes with $k \sim \xi^{-1}$ fall out of equilibrium at the Kibble-Zurek time

$$t_{\text{kz}} \sim \tau_0 \left(\frac{\tau_0}{\tau_Q} \right)^{-a\nu z / (a\nu z + 1)}, \quad \frac{a\nu z}{a\nu z + 1} \simeq 0.74, \quad (178)$$

where $\nu \simeq 0.63$. The correlation length at this time is

$$\ell_{\text{kz}} \sim \ell_0 \left(\frac{\tau_0}{\tau_Q} \right)^{-a\nu / (a\nu z + 1)}, \quad \frac{a\nu}{a\nu z + 1} \simeq 0.19. \quad (179)$$

Let us compare the t_{kz} and t_{cr} timescales. The Kibble-Zurek dynamics will begin to regulate the growth of critical fluctuations before the scaling behavior of the equation of state whenever $t_{\text{kz}} \gg t_{\text{cr}}$. In this limit $\Delta_s \rightarrow 0$ and the scaling structure of the equation of state is irrelevant, since the system falls out of equilibrium before reaching the detailed scaling regime. Comparing Eq. (178) and Eq. (174) we see that $t_{\text{kz}} \gg t_{\text{cr}}$ whenever Δ_s is less than a certain threshold Δ_{kz}

$$\Delta_s < \Delta_{\text{kz}} \equiv \lambda^{a\beta / (a\nu z + 1)}. \quad (180)$$

As shown in Fig. 5, for $\Delta_s < \Delta_{\text{kz}}$ the non-equilibrium length is set by ℓ_{kz} and the magnitude of the fluctuations is of order the equilibrium susceptibility at t_{kz} . Substituting numbers, with $a \simeq 1.12$, $z \simeq 3.96$, and $\beta = 0.32$, we find

$$\Delta_{\text{kz}} = 0.86 \left(\frac{\lambda}{0.2} \right)^{0.096}. \quad (181)$$

Clearly the strikingly small power, 0.096, makes the value Δ_{kz} remarkably insensitive to the value of λ . Thus, for realistic heavy-ion collisions with a finite λ , the detailed equilibrium scaling of the equation of state has a limited range of validity, $\Delta_{\text{kz}} \ll \Delta_s \ll 1$. Essentially, if one is close enough to the critical point, then the dynamics will always be out of equilibrium. Thus, to simulate the evolution of trajectories with $\Delta_s < \Delta_{\text{kz}}$, inputting an equation of state with the detailed scaling behavior (see Ref. [38]) into the hydrodynamic codes is not really necessary or sufficient. It is essential to simulate the non-equilibrium evolution of the system, along the lines of this work and Ref. [18].

Let us estimate the Kibble-Zurek timescale. We have defined a small parameter λ , and the three time scales in our problem,

$$\tau_0 \ll t_{\text{kz}} \ll \tau_Q, \quad (182)$$

are of relative size

$$\tau_0 \ll \tau_0 \lambda^{-0.74} \ll \tau_0 \lambda^{-1}. \quad (183)$$

Taking¹⁶ $\tau_0 \simeq 1.8 \text{ fm}$ and $\lambda = 0.2$, we find a relatively long time for t_{kz} :

$$1.8 \text{ fm} \ll 5.8 \text{ fm} \ll 8.9 \text{ fm}. \quad (184)$$

¹⁵ We have defined $\tau_R(\xi) \equiv 1/\Gamma_s(t, \xi^{-1})$ used in the body of the text, e.g. Eq. (132). The dynamical exponent $z = 4 - \eta$ is modified to $z = 3 - \eta$ in a more refined treatment where the conductivity λ_B is renormalized by critical fluctuations.

¹⁶ We have estimated the hadron density below using a thermal model. Then we multiplied the distance by the typical quasi particle velocity $\sqrt{3c_s^2}$ to arrive at this estimate.

Thus, if the system freezes out over a time of $t_{\text{kz}} \sim 5.8 \text{ fm}$, then the critical enhancement of fluctuations estimated below may be visible.

Similarly, the system has the length scales

$$\ell_0 \ll \ell_{\text{kz}} \ll \ell_{\text{max}}, \quad (185)$$

which are of relative size

$$\ell_0 \ll \ell_0 \lambda^{-0.18} \ll \ell_0 \lambda^{-1/2}. \quad (186)$$

The microscopic length ℓ_0 is of order the inter-particle spacing. For a hadronic gas with $n/s = 25$ and a chemical freezeout temperature $T \simeq 155 \text{ MeV}$ this length is approximately, $\ell_0 \simeq 1.2 \text{ fm}$. Taking $\lambda = 0.2$ we find that the three length scales are of order

$$1.2 \text{ fm} \ll 1.6 \text{ fm} \ll 2.7 \text{ fm}. \quad (187)$$

Comparing these numbers, we see that the correlation length at freezeout is at most twice the inter-particle spacing at these low densities.

Let us estimate the magnitude of the critical fluctuations when the Kibble-Zurek dynamics regulates the growth. The timescales and length-scales are set by the Kibble-Zurek time and length. Substituting t_{kz} from Eq. (178) into Eq. (173) (with $c_0 \sim f_\chi \sim 1$), we find that the magnitude of the fluctuations relative to our Poisson expectation are enhanced by

$$\left. \frac{N^{\hat{n}\hat{n}}(t_{\text{kz}}, \mathbf{k})}{n} \right|_{k \sim \ell_{\text{kz}}^{-1}} \sim \lambda^{-\gamma a / (a\nu z + 1)}. \quad (188)$$

Numerically for $\lambda = 0.2$ we find a somewhat anemic 80% enhancement

$$\left. \frac{N^{\hat{n}\hat{n}}(t_{\text{kz}}, \mathbf{k})}{n} \right|_{k \sim \ell_{\text{kz}}^{-1}} \sim 1.8 \left(\frac{\lambda}{0.2} \right)^{-0.37}. \quad (189)$$

This enhancement $\propto \lambda^{-0.37}$ is illustrated in Fig. 5, and is the largest one could reasonably expect in a heavy ion collision.

4. How this analysis can inform the experimental search for the critical point

We have analyzed the relevant length scales for the critical point search. In heavy ion collisions the longest wavelengths are long range in rapidity, and are described with hydrodynamics. These long wavelength modes, such as the elliptic and triangular flow, are not equilibrated and depend on the initial conditions. Only wavelengths smaller than a characteristic scale ℓ_{max} equilibrate during an expansion away from the critical point. Only modes with (wavelength) $\ll \ell_{\text{max}}$ can possibly exhibit critical properties. The typical wavelength for enhanced critical fluctuations is set by the Kibble-Zurek length ℓ_{kz} , and this length is only somewhat larger than the inter-particle spacing in practice. Such short lengths are associated with non-flow correlations. Thus, if critical fluctuations are to be seen then one must carefully examine the non-flow correlations to look for modifications as the mean baryon number to entropy ratio is changed in the event.

The current measurements of kurtosis are essentially a measure of the probability of finding a baryon at mid-rapidity while keeping the particle number (entropy) fixed. It seems

to us that the modifications of this quantity with beam energy are mostly a measurement of baryon transport in the initial state, and are perhaps unrelated to the critical fluctuations.

In order to measure the expected critical point signal, one should divide the system at different beam energies into different event classes with a specified n/s in a large mid-rapidity detector. (The proton to pion ratio can be used as a proxy for n/s .) If the system passes close to the critical point, the short range (connected) two point functions should change as the n/s event class is scanned. These changes in the two point functions should be largely independent of centrality and beam energy, but should depend only on the mean n/s of the event class. The presence of a critical point leads to short range spatial correlations of size of order ℓ_{kz} . In momentum space this corresponds to a momentum difference of order $\Delta p \sim \hbar/\ell_{kz} \sim 50$ MeV. Thus, the presence of a critical point there will enhance the short-range, almost HBT-like, correlations.

Any non-monotonic changes in the non-flow correlation strength in this fixed momentum range with the mean n/s would certainly be remarkable. We plan to investigate such correlations in future work, and encourage our experimental colleagues to do the same.

ACKNOWLEDGMENTS

We thank Aleksas Mazeliauskas for collaboration during the initial stages of this project. We are grateful to Jiunn-wei Chen, Prithwish Tribedy, Xiaofeng Luo, Misha Stephanov for helpful conversations. This work is supported by JSPS KAKENHI Grant Number JP18K13538 (Y.A.) and by the U.S. Department of Energy, Office of Science, Office of Nuclear Physics, within the framework of the Beam Energy Scan Theory (BEST) Topical Collaboration (Y.Y.) and grants Nos. DE-FG-02-08ER41450 (D.T. , F.Y) and DE-SC0011090 (Y.Y)

Appendices

A. THE ISING EQUATION OF STATE AND CORRELATION LENGTH

In this section we will parametrize the Ising equation of state with the familiar (R, θ) form.

1. Preliminaries

The free energy is the log of the partition function¹⁷

$$F(T, H) = -T \frac{\log Z(T, H)}{V}, \quad \text{with} \quad dF = -SdT - \psi dH, \quad (190)$$

and thus

$$\frac{d \log Z(T, H)}{V} = \frac{\mathcal{E}}{T^2} dT + \frac{\psi}{T} dH, \quad (191)$$

where the energy density is $\mathcal{E} = F - T \frac{\partial F}{\partial T}$. Near the critical point $Z(T, H)$ is the product of a regular contribution and a singular contribution, $Z_{\text{reg}} \times Z_{\text{sing}}$. The regular part is expanded in a Taylor series near the critical point, keeping only linear terms

$$\frac{\Delta \log Z_{\text{reg}}}{V} = \mathcal{E}_c \frac{\Delta T}{T_c^2} = -\frac{\Delta F_{\text{reg}}}{T_c}, \quad \Delta F_{\text{reg}} = S_c \Delta T. \quad (192)$$

Due to the Z_2 symmetry of the Ising model, the regular part starts as H^2 which can be neglected close to the critical point. Given Eq. (191) and Eq. (192) the singular contribution Z_{sing} satisfies

$$d \log Z_{\text{sing}} = -\frac{dF_{\text{sing}}}{T_c} = \epsilon dr + \psi dh, \quad \frac{dF_{\text{sing}}}{T_c} = -s dr - \psi dh, \quad (193)$$

where we have defined $r = (T - T_c)/T_c$, $\epsilon = (\mathcal{E} - \mathcal{E}_c)/T_c$, $h = H/T_c$, and $s = S(T, H) - S_c$. Thus, near the critical point we have $\epsilon = s$ which follows from the definition of \mathcal{E} , ϵ , and the decomposition of $Z = Z_{\text{reg}} \times Z_{\text{sing}}$ into regular and singular parts.

The free energy F is the Legendre transform of the Gibbs free energy $G(T, \psi) = F + \psi H$. The singular part satisfies

$$\log Z_{\text{sing}}(r, h) = -\frac{G_{\text{sing}}(r, \psi)}{T_c} + \psi h, \quad (194)$$

and the reduced magnetic field h is related to $G_{\text{sing}}(r, \psi)/T_c$ by the thermodynamic relations, $h = (\partial(G_{\text{sing}}/T_c)/\partial\psi)_r$.

¹⁷ Relative to Ref. [25], but in accord with Ref. [26], we have reversed the roles of F (what we call the free energy) and G (what we call the Gibbs free energy)

2. The (R, θ) parameterization

Following previous authors [25, 26], we parametrize the Ising equation of state outside of the coexistence region with two auxiliary variables (R, θ) with $\theta^2 \leq \theta_0^2$

$$r = (1 - \theta^2)R, \quad (195)$$

$$\frac{h}{h_0} = c_h \theta \left(1 - \frac{\theta^2}{\theta_0^2}\right) R^{\beta\delta}. \quad (196)$$

Then the equation of state takes the form [26]

$$\frac{\psi}{\mathcal{M}_0} = c_{\mathcal{M}} \theta R^\beta, \quad (197)$$

where δ and β are critical exponents. θ_0 demarcates the boundary of the coexistence region and is approximately¹⁸

$$\theta_0 = \left(\frac{\delta - 3}{(\delta - 1)(1 - 2\beta)} \right)^{1/2} \simeq 1.166. \quad (198)$$

As discussed in Sect. II A, the dimensionful constants $M_0 h_0$ and \mathcal{M}_0 are chosen conventionally to be (n_c, s_c) so that mapping matrix M_b^A is of order unity. The constants c_h and $c_{\mathcal{M}}$ will be chosen to maintain the convenient normalization conventions adopted in Sect. II C: namely that on coexistence line $\psi/\mathcal{M}_0 = |r|^\beta$ and $\epsilon/(\mathcal{M}_0 h_0) = -|r|^{1-\alpha}$. Thus

$$c_{\mathcal{M}} = \frac{(\theta_0^2 - 1)^\beta}{\theta_0} \simeq 0.6145, \quad (199)$$

and $c_{\mathcal{M}} c_h$ is given below in Eq. (210).

The dimensionless scaling variable θ is directly related to the scaling variable used in¹⁹ Ref. [32]

$$z = \left(\frac{r}{r_S} \right) \left(\frac{h_S}{h/(c_h h_0)} \right)^{1/\beta\delta} = 1.901 \frac{(1 - \theta^2)}{[\theta(1 - (\theta/\theta_0)^2)]^{1/\beta\delta}}, \quad (200)$$

where we defined

$$r_S = \frac{\theta_0^2 - 1}{\theta_0^{1/\beta}} \simeq 0.225, \quad \text{and} \quad h_S = \frac{\theta_0^2 - 1}{\theta_0^2} = 0.265. \quad (201)$$

Following Ref. [25], we can integrate the equation of state, Eq. (197), to determine the singular part of the grand sum, $\log Z(r, h)$, which subsequently determines all thermodynamic quantities and susceptibilities through differentiation. Parametrizing G_{sing}/T_c as

$$\frac{1}{h_0 \mathcal{M}_0} \frac{G_{\text{sing}}(r, \psi)}{T_c} = c_h c_{\mathcal{M}} R^{2-\alpha} g(\theta), \quad (202)$$

¹⁸ The differences between our parameterization (taken from Ref. [26]) and the parameterization used in Ref. [25] are minor. We have neglected the fifth order term in the polynomial expansion of $\tilde{h}(\theta) \simeq \theta(1 - \theta^2/\theta_0^2)$, and taken an analytic expression (valid to ϵ^2 in the ϵ expansion) for the first zero θ_0 of $\tilde{h}(\theta)$ [26]. With this simplified parametrization the specific heat C_M is only a function of R and the susceptibilities take a compact form. The numerical accuracy of this parametrization is more than sufficient for heavy ion physics.

¹⁹ Here our $(h/c_h h_0)$ and h_S are denoted by H and H_0 respectively by Ref. [32]

a differential equation is easily obtained for $g(\theta)$:

$$(1 - \theta^2)g'(\theta) + 2(2 - \alpha)\theta g(\theta) = (2\beta\theta^2 + (1 - \theta^2))\theta(1 - (\theta/\theta_0)^2)^2. \quad (203)$$

Integrating the differential equation we find

$$g(\theta) = \frac{(2\beta - 1)(\theta^2 - 1)^2}{2\alpha\theta_0^2} + \frac{(\theta^2 - 1)((1 - 2\beta)\theta_0^2 + 4\beta - 1)}{2(\alpha - 1)\theta_0^2} - \frac{\beta(\theta_0^2 - 1)}{(\alpha - 2)\theta_0^2}, \quad (204)$$

up to a homogeneous solution which does not contribute to the singular behavior [25].

From these expressions first derivatives can be obtained

$$\begin{pmatrix} -s & h \end{pmatrix} = \frac{\partial(G_{\text{sing}}/T_c)}{\partial(r, \psi)} = \frac{\partial(G_{\text{sing}}/T_c)}{\partial(R, \theta)} \begin{pmatrix} \partial(R, \theta) \\ \partial(r, \psi) \end{pmatrix}, \quad (205)$$

where in practice this Jacobian matrix is evaluated through its inverse

$$\begin{pmatrix} \partial(R, \theta) \\ \partial(r, \psi) \end{pmatrix} = \begin{pmatrix} \partial(r, \psi) \\ \partial(R, \theta) \end{pmatrix}^{-1}. \quad (206)$$

The singular entropy density and the singular energy density take the form

$$\frac{\epsilon}{\mathcal{M}_0 h_0} = \frac{s}{\mathcal{M}_0 h_0} = c_{\mathcal{M}} c_h R^{1-\alpha} f_\epsilon(\theta) \quad (207)$$

with

$$f_\epsilon(\theta) = \frac{\beta(1 - \delta)(-(1 - \alpha)(2\beta - 1)\theta^2 + \alpha + 2\beta - 1)}{2(1 - \alpha)\alpha}, \quad (208)$$

$$\simeq 1.496 - 1.951\theta^2. \quad (209)$$

From our requirement that on the coexistence line that $\epsilon/(\mathcal{M}_0 h_0) = -|r|^{1-\alpha}$ we find

$$c_{\mathcal{M}} c_h = -\frac{(\theta_0^2 - 1)^{1-\alpha}}{f_\epsilon(\theta_0)} \simeq 0.3486. \quad (210)$$

In a similar way the susceptibility matrix can be computed by taking second derivatives of the partition function, yielding

$$\frac{C_M}{\mathcal{M}_0 h_0} = c_{\mathcal{M}} c_h \frac{\gamma(\gamma - 1)}{2\alpha} R^{-\alpha}, \quad (211a)$$

$$\frac{\chi}{(\mathcal{M}_0/h_0)} = \frac{c_{\mathcal{M}}}{c_h} \left[1 + (2\beta\delta - 3)(\delta - 1)\theta^2/(\delta - 3) \right]^{-1} R^{-\gamma}, \quad (211b)$$

$$\frac{C_H}{\mathcal{M}_0 h_0} = c_{\mathcal{M}} c_h \frac{\gamma}{2\alpha} \left[\frac{(2\beta - 1)(\delta - 1)(\beta(\delta + 3) - 3)\theta^2 + (\delta - 3)(\gamma - 1)}{(\delta - 1)(2\beta\delta - 3)\theta^2 + (\delta - 3)} \right] R^{-\alpha}. \quad (211c)$$

It is particularly noteworthy that C_M is independent of the angle θ .

3. The correlation length

To evaluate the correlation length we used the numerical data from Engels, Fromme and Seniuch (EFS) [32] which is expressed in terms of the scaling variable z given in Eq. (200). The correlation length takes the scaling form

$$\xi(h, z) = \left(\frac{h/(c_h h_0)}{h_S} \right)^{-\nu/\beta\delta} g_\xi(z). \quad (212)$$

where $g_\xi(z)$ is a universal function (up to its normalization), which was determined numerically through precise simulations of the Ising model. Even its normalization is not independent of the non-universal parameters, \mathcal{M}_0 and h_0 , introduced previously.

Since $g_\xi(z) \propto z^{-\nu}$ for z large, the correlation length at zero field and $T > T_c$ behaves as

$$\xi \xrightarrow{z \rightarrow \infty} \xi_+ r^{-\nu}, \quad (213)$$

where we have used the definition of z given in Eq. (200). The length scale ξ_+ is not independent of \mathcal{M}_0 and h_0 , but is fixed from the scaling form the free energy

$$-\frac{F_{\text{sing}}}{T_c} = \frac{\log Z_{\text{sing}}(r, h)}{V} = \xi^{-d} \mathcal{F}_{\text{sing}}(z), \quad (214)$$

where $d = 3$ notates the number of spatial dimensions, and $\mathcal{F}_{\text{sing}}(z)$ is a universal function. Comparison with Eq. (202) suggests that $\mathcal{M}_0 h_0 (\xi_+)^d$ should be a universal constant [26]. Indeed, EFS relate ξ_+ to the parameters of the equation of state, \mathcal{M}_0 and h_0 , introduced above. Translating their ratio into the current notation we have²⁰

$$(c_{\mathcal{M}} c_h) \mathcal{M}_0 h_0 \xi_+^d = 0.1231. \quad (216)$$

In EFS, the numerical data for a normalized $g_\xi(z)$ is presented by comparing it to the scaling function of the susceptibility. Specifically, the susceptibility χ (see Eq. (211b)) is written

$$\chi = \frac{1}{h_S} \left(\frac{h/(c_h h_0)}{h_S} \right)^{1/\delta-1} f_\chi(z), \quad (217)$$

where h_S and its relation to the notation of EFS is given in Eq. (200) and the corresponding footnote. $f_\chi(z)$ has the asymptotic form

$$f_\chi \xrightarrow{z \rightarrow +\infty} R_\chi z^{-\gamma}, \quad (218)$$

with $R_\chi \simeq 1.723$. $g_\xi(z)$ is normalized and scaled by $f_\chi(z)$

$$g_\xi(z) = g_\xi(0) (f_\chi(z))^{1/2} \left(\frac{\hat{g}_\xi^2(z)}{f_\chi(z)} \right)^{1/2}. \quad (219)$$

²⁰ They define the parameters B and C_+ which in the current notation read:

$$B = \frac{\theta_0}{(\theta_0^2 - 1)^\beta} (c_{\mathcal{M}} \mathcal{M}_0) \simeq 1.6274 (c_{\mathcal{M}} \mathcal{M}_0), \quad C_+ = \frac{c_{\mathcal{M}} \mathcal{M}_0}{c_h h_0}. \quad (215)$$

They numerically determine the amplitude ratio $Q_c = B^2 (\xi_+)^d / C_+ = 0.326$ which determines Eq. (216).

We fit the numerical data in Fig. 11 of EFS with

$$\frac{\hat{g}_\xi^2(z)}{f_\chi(z)} = \frac{(u_+ + u_-) - (u_- - u_+) \tanh((z - x_0)/\sigma)}{2((z - x_0)^2 + 1)^{\eta\nu/2}}, \quad (220)$$

which has the correct asymptotics

$$\frac{\hat{g}_\xi^2(z)}{f_\chi(z)} \xrightarrow{z \rightarrow \pm\infty} u_\pm z^{-\eta\nu/2}. \quad (221)$$

The parameters are u_+ , u_- , and σ from the fit are

$$u_+ = 4.133, \quad u_- = 5.32, \quad \sigma = 3, \quad x_0 = 0.3431. \quad (222)$$

The value $x_0 = 0.3431$ is constrained by the universality requirement that at $z = 0$ we have $\hat{g}_\xi^2/f_\chi = \delta$. The slight deviation in our fitted values of u_+ and u_- from the asymptotic values quoted by EFS ($u_+ = 4.001$ and $u_+/u_- \simeq 0.75$ respectively) stems from a desire to have a somewhat better fit over the full range in z . Finally, with the functional form given in Eq. (220) and the normalization in Eq. (216), the value of $g_\xi(0)$ of zero can be determined

$$g_\xi(0) = \frac{0.4838}{(c_{\mathcal{M}} c_h \mathcal{M}_0 h_0)^{1/d}}, \quad (223)$$

where we have unraveled the nested definitions to establish that $\xi_+ = g_\xi(0) r_S^\nu (u_+ R_\chi)^{1/2}$.

Summarizing, we use Eqs. (212), (219), (220), and (223) to evaluate the correlation length for any given value of h, r .

-
- [1] H.-T. Ding, F. Karsch, and S. Mukherjee, *Int. J. Mod. Phys. E* **24**, 1530007 (2015), [arXiv:1504.05274 \[hep-lat\]](#).
 - [2] M. A. Stephanov, *Prog.Theor.Phys.Suppl.* **153**, 139 (2004), [arXiv:hep-ph/0402115 \[hep-ph\]](#).
 - [3] M. Stephanov, PoS **LAT2006**, 024 (2006), [arXiv:hep-lat/0701002 \[hep-lat\]](#).
 - [4] K. Fukushima and T. Hatsuda, *Rept.Prog.Phys.* **74**, 014001 (2011), [arXiv:1005.4814 \[hep-ph\]](#).
 - [5] “Studying the phase diagram of qcd matter at rhic,” (2014), https://drupal.star.bnl.gov/STAR/files/BES_WP1I_ver6.9_Cover.pdf.
 - [6] X. Luo and N. Xu, *Nucl. Sci. Tech.* **28**, 112 (2017), [arXiv:1701.02105 \[nucl-ex\]](#).
 - [7] M. A. Stephanov, K. Rajagopal, and E. V. Shuryak, *Phys.Rev.Lett.* **81**, 4816 (1998), [arXiv:hep-ph/9806219 \[hep-ph\]](#).
 - [8] M. A. Stephanov, K. Rajagopal, and E. V. Shuryak, *Phys.Rev.* **D60**, 114028 (1999), [arXiv:hep-ph/9903292 \[hep-ph\]](#).
 - [9] B. Berdnikov and K. Rajagopal, *Phys.Rev.* **D61**, 105017 (2000), [arXiv:hep-ph/9912274 \[hep-ph\]](#).
 - [10] S. Mukherjee, R. Venugopalan, and Y. Yin, *Phys. Rev.* **C92**, 034912 (2015), [arXiv:1506.00645 \[hep-ph\]](#).
 - [11] Y. Akamatsu, A. Mazeliauskas, and D. Teaney, *Phys. Rev.* **C95**, 014909 (2017), [arXiv:1606.07742 \[nucl-th\]](#).
 - [12] T. Kibble, *Physics Reports* **67**, 183 (1980).

- [13] W. H. Zurek, *Nature (London)* **317**, 505 (1985).
- [14] W. H. Zurek, *Phys. Rept.* **276**, 177 (1996), [arXiv:cond-mat/9607135 \[cond-mat\]](#).
- [15] A. Chandran, A. Erez, S. S. Gubser, and S. L. Sondhi, *Phys. Rev. B* **86**, 064304 (2012).
- [16] S. Mukherjee, R. Venugopalan, and Y. Yin, *Phys. Rev. Lett.* **117**, 222301 (2016), [arXiv:1605.09341 \[hep-ph\]](#).
- [17] A. Andreev, *Zhurnal Eksperimental'noj i Teoreticheskoy Fiziki* **75**, 1132 (1978).
- [18] M. Stephanov and Y. Yin, (2017), [arXiv:1712.10305 \[nucl-th\]](#).
- [19] S. Pratt, J. Kim, and C. Plumberg, (2017), [arXiv:1712.09298 \[nucl-th\]](#).
- [20] Y. Akamatsu, A. Mazeliauskas, and D. Teaney, *Phys. Rev.* **C97**, 024902 (2018), [arXiv:1708.05657 \[nucl-th\]](#).
- [21] J. I. Kapusta and J. M. Torres-Rincon, *Phys. Rev.* **C86**, 054911 (2012), [arXiv:1209.0675 \[nucl-th\]](#).
- [22] C. Plumberg and J. I. Kapusta, *Phys. Rev.* **C95**, 044910 (2017), [arXiv:1702.01368 \[nucl-th\]](#).
- [23] M. Sakaida, M. Asakawa, H. Fujii, and M. Kitazawa, *Phys. Rev.* **C95**, 064905 (2017), [arXiv:1703.08008 \[nucl-th\]](#).
- [24] M. Nahrgang, M. Bluhm, T. Schafer, and S. A. Bass, *Nucl. Phys.* **A967**, 824 (2017).
- [25] C. Nonaka and M. Asakawa, *Phys. Rev.* **C71**, 044904 (2005), [arXiv:nucl-th/0410078 \[nucl-th\]](#).
- [26] A. Onuki, *Phase Transition Dynamics* (Cambridge University Press, 2002).
- [27] See for example sections 16, 111, and 112: L. Landau and E. M. Lifshitz, *Statistical Physics, Part 1*, Course of Theoretical Physics, Vol. 5 (Elsevier Science, 2013). Note that S in the non-relativistic literature typically denotes the entropy per particle S/N .
- [28] L. P. Kadanoff and P. C. Martin, *Annals of Physics* **24**, 419 (1963).
- [29] L. Landau, E. Lifshitz, and L. Pitaevskij, *Statistical Physics: Part 2 : Theory of Condensed State*, Landau and Lifshitz Course of theoretical physics (Oxford, 1980).
- [30] M. Combescot, M. Droz, and J. M. Kosterlitz, *Phys. Rev. B* **11**, 4661 (1975).
- [31] J. Zinn-Justin, *Quantum Field Theory and Critical Phenomena*, International series of monographs on physics (Clarendon Press, 2002).
- [32] J. Engels, L. Fromme, and M. Seniuch, *Nucl. Phys.* **B655**, 277 (2003), [arXiv:cond-mat/0209492 \[cond-mat\]](#).
- [33] L. Ryzhik, G. Papanicolaou, and J. B. Keller, *Wave Motion* **24**, 327 (1996).
- [34] P. C. Hohenberg and B. I. Halperin, *Rev. Mod. Phys.* **49**, 435 (1977).
- [35] D. Son and M. Stephanov, *Phys.Rev.* **D70**, 056001 (2004), [arXiv:hep-ph/0401052 \[hep-ph\]](#).
- [36] M. Natsuume and T. Okamura, *Phys. Rev.* **D83**, 046008 (2011), [arXiv:1012.0575 \[hep-th\]](#).
- [37] K. Kawasaki, *Annals of Physics* **61**, 1 (1970).
- [38] P. Parotto, M. Bluhm, D. Mroczek, M. Nahrgang, J. Noronha-Hostler, K. Rajagopal, C. Ratti, T. Schafer, and M. Stephanov, (2018), [arXiv:1805.05249 \[hep-ph\]](#).